Modeling and analyzing competitive epidemic diseases with partial and waning virus-specific and cross-immunity

Modeling and analyzing competitive epidemic diseases with partial and waning virus-specific and cross-immunity*

Lorenzo Zino[a,b,*], Mengbin Ye[b], Brian D.O. Anderson[c]

[a] *Department of Electronics and Telecommunications, Politecnico di Torino, Corso Duca Degli Abruzzi 24, 10129 Torino, Italy*
[b] *Centre for Optimisation and Decision Science, Curtin University, Perth, Australia*
[c] *School of Engineering, Australian National University, Canberra, Australia*

Abstract

In this paper, we consider a novel mathematical modeling framework for the spread of two competitive diseases in a well-mixed population. The proposed framework, which we term a bivirus SIRIS model, encapsulates key real-world features of natural immunity, accounting for different levels of (partial and waning) virus-specific and cross protection acquired after recovery. Formally, the proposed framework consists of a system of coupled nonlinear ordinary differential equations that builds on a classical bivirus susceptible–infected–susceptible model by means of the addition of further states to account for (temporarily) protected individuals. Through the analysis of the proposed framework and of two specializations, we offer analytical insight into how natural immunity can shape a wide range of complex emergent behaviors, including eradication of both diseases, survival of the fittest one, or even steady-state co-existence of the two diseases.

Keywords: epidemic model, compartmental model, competitive virus, nonlinear, ordinary differential equations

1. Introduction

Mathematical models have emerged as powerful frameworks to predict the spread of epidemic diseases, assess the effectiveness of different intervention policies, and, ultimately, derive tools to help assist public health authorities in their decision-making during an health crisis [1–4]. In their original formulations, these models consider a single disease (to which we shall refer as a *virus*) spreading in a population. Recently, models considering the simultaneous spread of multiple competitive viruses have being developed, for which it is assumed that individuals cannot contract multiple diseases at the same time [5–9]. These models allow study of antagonistic viral interference —which often occurs between respiratory viruses [10–12]— and the competition between multiple strains of the same virus —e.g., coronaviruses [13].

1.1. Literature review

The literature on competitive viruses mostly focuses on two viruses that follow a susceptible–infected–susceptible (SIS) epidemic progression, relying on the simplifying assumption that individuals become immediately susceptible again to both diseases after recovery [5–9]. The theoretical analysis of such models, which are termed bivirus SIS models, has established that two scenarios are possible: either both diseases are eradicated, or the fitter virus —technically, the one with largest basic reproduction number— becomes endemic [6]. Therefore, persistent co-existence of the two viruses is not a feasible emergent behavior of such a model, unless considering the non-generic scenarios in which the two viruses have exactly the same basic reproduction number, or assuming more complex scenarios in which the population is spatially distributed and thus interacts via a network structure [14], or the spread is driven by a complex (nonlinear) contagion mechanisms [15].

Nevertheless, the medical literature provides strong evidence that persistent co-existence of multiple competing viruses is not only possible, but is also a very common fact, even in a well-mixed population. This is the case, e.g., with viruses causing seasonal flu and the common cold (RSVs), which are in competition but are observed spreading concurrently [10, 11, 16]. Interestingly, among the various factors that favor the emergence and persistence of such co-existence of multiple viruses, the medical literature suggests that natural immunity may play a key role [17].

Indeed, natural immunity is a very complex phenomenon. In fact, recovery from a disease often yields some level of protection against re-infection with the same virus and, in some cases, it also grants a level of cross-immunity against other competitive viruses. This is the case, e.g., with orthopoxviruses —including variola major, variola minor, and monkeypox— which provide al-

*M. Ye is supported by the Western Australian Government through the Premier's Science Fellowship Program and the Defence Science Centre.

*Corresponding author. Email: lorenzo.zino@polito.it

most complete virus-specific and cross-immunity [18, 19], or different strains of RSVs [17] and COVID-19 [20–22], for which however the protection against re-infection is only partial. On the other hand, not all competitive viruses provide cross-immunity: there is no evidence that recovery from influenza grants protection from RSVs [10], or of cross-immunity for different strains of rhinoviruses [23]. Moreover, depending on the virus, the (possibly partial) protection gained after recovery may be permanent (such as for orthopoxviruses [18]), or may vanish in time (such as for COVID-19 [20–22]).

Despite such a pervasive presence, natural immunity is typically overlooked or oversimplified in mathematical multi-virus models. In fact, most of the analytically-tractable models for competing viruses that account for immunity use a susceptible–infected–removed (SIR) model [24–26], where natural immunity is assumed to be perfect and permanent for all viruses, while all aspects of immunity discussed in the above have been typically investigated only via numerical simulations [27, 28].

Here, we fill in this gap by proposing an analytically-tractable mathematical model —called the bivirus SIRIS model— in which two competitive viruses spread in a population with specific focus on the different aspects of natural immunity. In particular, building on the preliminary effort in [29], we expand a classical bivirus SIS model [9] by incorporating two additional compartments to account for individuals who have recovered from the two viruses and a set of tunable parameters to capture the key differences between virus-specific and cross immunity, and to account for the waning nature of immunity. Formally, the model consists of a system of coupled nonlinear ordinary differential equations (ODEs), which capture the evolution of the fraction of population belonging to each compartment.

1.2. Paper contribution

The main contributions of this paper build on the preliminary findings from [29] and extend them along multiple directions, including the development of novel theoretical findings, which rely on the use of new and nontrivial technical arguments, as well as the expansion of the model motivation and the discussion of the results. Specifically, the contributions of this paper are five-fold, and can be summarized as follows:

- We formalize a single-virus implementation of the SIRIS model, which serves as a baseline for all further studies, and we analyze its behavior. The novel results relative to [29] are Theorems 1 and 2.
- After illustrating our bivirus SIRIS model, firstly proposed in [29], we present some novel general results on its asymptotic behavior. Specifically, we establish conditions on the parameters for which the disease-free equilibrium (DFE) is globally asymptotically stable, and thus both viruses are eradicated (Theorem 3). Then, we focus on the behavior of the system when the DFE is not stable, characterizing the endemic equilibria (EEs) in which a single virus survives —termed boundary endemic equilibria (BEEs)— and proving that co-existence equilibria (CEEs), if they exist, are finite in number and nondegenerate (Propositions 5 and 6, respectively). Technically, the high-dimensionality and nonlinearity of the system of ODEs call for the use of an array of different analytical methods, ranging from classical linearization techniques to tools borrowed from systems theory [30, 31] and differential geometry [32, 33].
- We analyze a first specialization of the model involving a scenario of non-waning but partial immunity, which is a proxy for several real-world multi-strain diseases where immunity wanes at a much slower time-scale than the competition between different strains. For this specialization, we offer two sets of novel analytical results. First, we characterize its transient behavior, which we bound in terms of simpler SIS-like equations (Proposition 9). Second, we expand the results in [29] —which only focus on existence of EEs— by providing a complete characterization of the asymptotic behavior of the model (Theorem 4), including the analysis of the stability of the healthy manifold and the study of the non-generic case in which the two viruses have the same contagiousness, which gives rise to a line segment of equilibria.
- We analyze a second specialization of the model in which recovery from a virus grants waning virus-specific immunity but not cross immunity. By combining tools from systems theory and differential geometry, we derive an array of novel analytical insights, expanding the analysis of BEEs (Theorem 5) and CEEs (Propositions 13 and 14), and demonstrating a key novel finding: for a certain range of the parameter values, CEEs exist. Such a conclusion is consistent with real-life observations [10, 11, 16, 34], and may provide analytical support for the discussion on the role of immunity on co-existence between different competing viruses, which is a phenomenon often observed in the medical literature [17], but one that cannot be predicted using the simpler SIS bivirus model [6].
- Importantly, we extend the discussion on the model motivation and on the implications of our theoretical findings with respect to the medical literature.

The rest of the paper is organized as follows. In Section 2, we present the single-virus model and our results on its analysis. In Section 3, we introduce our general formalism. In Section 4, we present our results on the model and on its equilibria. Then, the two specializations of the model are studied, with results reported in Sections 5 and 6, respectively. Section 7 concludes the paper.

2. Single-virus SIRIS Model

Here, we present a single-virus implementation of the SIRIS model, which encapsulates partial and waning natural immunity. Through its analysis, we bound its temporal evolution by means of simpler SIS models, and we determine its asymptotic behavior, i.e., whether the disease is eradicated or becomes endemic. These results will serve as a baseline for our study of the bivirus SIRIS model.

2.1. Model

We extend the classical scalar SIS and SIR models [3] by assuming that recovery provides only partial (and possibly waning) immunity. Hence, recovered individuals may further transition to either the infected or the susceptible state. We consider a fully-mixed population, and we denote by $w(t)$ the fraction of the population susceptible to the virus at (continuous) time $t \geq 0$, $x(t)$ the fraction of infected population, and $y(t)$ the fraction of population who recovered from it and is (partially) immune to re-infection. Noting that $w(t) = 1-x(t)-y(t)$, we can reduce the state space of the system to the two dimensional vector $(x, y) \in \mathcal{D}$, with $\mathcal{D} := \{(x, y) \in [0, 1]^2 : x + y \leq 1\}$. We consider the following planar system of ODEs:

$$\dot{x} = -\mu x + \lambda x(1 - x - (1 - \alpha)y), \tag{1a}$$

$$\dot{y} = \mu x - \nu y - \alpha\lambda xy, \tag{1b}$$

Thus, an individual infected with the virus recovers at a rate $\mu > 0$. Once recovered, the individual acquires partial immunity, which is captured by the parameter $\alpha \in [0, 1]$: $\alpha = 1$ models absence of immunity, $\alpha = 0$ models perfect immunity. Such a parameter affects the contagion rate as a multiplicative factor. Namely, while susceptible individuals (the corresponding fraction being equal to $1 - x - y$) are infected by coming into contact with infected individuals with contagion rate $\lambda > 0$, those that are (partially) immune are infected with contagion rate reduced to $\alpha\lambda$. Finally, natural immunity wanes at a rate $\nu \geq 0$, and the individual becomes susceptible again. Note that here we allow ν to be equal to 0, capturing the limiting case in which immunity does not wane, being the case, e.g., for orthopoxviruses [18].

2.2. Results

Before presenting our results on the single-virus SIRIS model, we introduce some terminology.

Definition 1. *The healthy manifold is defined as* $\mathcal{H} := \{(x, y) \in \mathcal{D} : x = 0\}$*, and the disease-free equilibrium (DFE) as* $(x, y) = \mathbf{0}$*. Given* $(\bar{x}, \bar{y}) \in \mathcal{D}$*, a fixed point of Eq. (1),* $(\bar{x}, \bar{y})$ *is an endemic equilibrium (EE) if* $\bar{x} > 0$*.*

Proposition 1. *The domain* $\mathcal{D}$ *and the healthy manifold* $\mathcal{H}$ *are positively invariant for Eq. (1). Moreover, if* $(x(0), y(0)) \in \mathcal{H}$ *and* $\nu > 0$*, then* $\lim_{t\to\infty}(x(t), y(t)) = \mathbf{0}$*.*

Proof. The domain $\mathcal{D}$ is compact and convex and Eq. (1) is Lipschitz-continuous. Hence, Nagumo's Theorem can potentially be applied [35]. We are left with checking the direction of the vector field at the boundaries of $\mathcal{D}$. We immediately observe that $\dot{x} = 0$ for $x = 0$; $\dot{y} = \nu x \geq 0$, for $y = 0$. Finally, for $x = 1 - y$, we observe that the field points towards the interior, as $\dot{x} + \dot{y} = -\nu y \leq 0$. Hence, Nagumo's Theorem implies positive invariance of $\mathcal{D}$. Positive invariance of $\mathcal{H}$ can be easily checked, since $\dot{x} = 0$ for all $(x, y) \in \mathcal{H}$. Finally, given $(x(0), y(0)) = (0, y_0) \in \mathcal{H}$, Eq. (1) can be solved analytically, obtaining $(x(t), y(t)) = (0, y_0 e^{-\nu t})$, which yields the claim. □

Now, we present a general result, which provides upper and lower bounds on the temporal evolution of the epidemic process in terms of simpler epidemic models.

Proposition 2. *Let* $(x(t), y(t))$ *be the solution of Eq. (1) with initial condition* $(x(0), y(0))$*. Then there holds* $\underline{z}(t) \leq x(t) \leq \overline{z}(t)$*, where* $\underline{z}(t)$ *and* $\overline{z}(t)$ *are the solutions of the Cauchy problems*

$$\dot{z} = -\mu z + \alpha\lambda z(1 - z), \qquad z(0) = x(0) \tag{2}$$

and

$$\dot{z} = -\mu z + \lambda z(1 - z), \qquad z(0) = x(0), \tag{3}$$

respectively which can be computed explicitly, obtaining $\underline{z}(t) = \frac{\alpha\lambda-\mu}{\alpha\lambda+(\alpha\lambda-\mu)\frac{\alpha\lambda(1-x(0))-\mu}{(\alpha\lambda-\mu)x(0)}\exp\{-(\alpha\lambda-\mu)t\}}$ *and* $\overline{z}(t) = \frac{\lambda-\mu}{\lambda+(\lambda-\mu)\frac{\lambda(1-x(0))-\mu}{(\lambda-\mu)x(0)}\exp\{-(\lambda-\mu)t\}}$*. Moreover, inequalities are strict for any finite* $t > 0$*, if* $\alpha \in (0, 1)$*,* $x(0) + y(0) < 1$*, and* $y(0) > 0$*.*

Proof. For the upper bound in Eq. (2), we observe from Eq. (1a) that $\dot{x} = -\mu x + \lambda x(1 - x - (1 - \alpha)y) = -\mu x + \lambda xw + \alpha\lambda xy \geq -\mu x + \lambda\alpha x(1 - x)$, being $w, x, y \in [0, 1]$ (Proposition 1), and $\alpha \in [0, 1]$, which yields the claim. For the upper bound in Eq. (3), we observe from Eq. (1a) that $\dot{x} = -\mu x + \lambda x(1 - x - (1 - \alpha)y) \leq -\mu x + \lambda x(1 - x)$, being $y \in [0, 1]$ (Proposition 1), which yields the claim.

Finally, to prove strictness, we proceed as follows. From Eq. (1), we observe that $\dot{y} \geq -(\nu + \alpha\lambda)y$ and $\dot{w} \geq -\lambda w$. Hence, Gronwall's inequality [30] yields $y(t) \geq y(0)\exp\{-(\nu + \alpha\lambda)t\}$ and $w(t) \geq (1 - x(0) - y(0))\exp\{-\lambda t\}$. Hence, if $x(0) + y(0) < 1$ and $y(0) > 0$, then $w(t)$ and $y(t)$ are always strictly positive for any finite $t \geq 0$. As a consequence, under these conditions and with the further assumption that $\alpha \in (0, 1)$, the inequalities on $\dot{x}$ are strict, which implies that the inequalities on $x(t)$ are strict too, for any finite strictly positive time $t > 0$. □

Note that Eqs. (2) and (3) are each equations of a simple SIS system; thus the proposition shows that an SIRIS model has a behavior in some sense between the behaviors of two SIS models, which are determined by the SIRIS model. Note that $\alpha = 1$ models the absence of immunity, and then the two SIS models in fact coincide.

The (non-strict) inequalities established in the proposition obviously will continue to hold when $t \to \infty$, and we also know what the limits of $\underline{z}(t)$ and $\bar{z}(t)$ are, depending as they do on the values of $\mu/\alpha\lambda$ and μ/λ. This allows us to state the following corollary.

Corollary 1. *If $\lambda/\mu \leq 1$, then $\lim_{t\to\infty} x(t) = 0$. If $\lambda\alpha/\mu > 1$, then, for any $\sigma > 0$ there exists a finite constant $T_\sigma \geq 0$ such that, for any $t \geq T_\sigma$, there holds $x(t) \in [\frac{\lambda\alpha-\mu}{\lambda\alpha} - \sigma, \frac{\lambda-\mu}{\lambda} + \sigma]$.*

In the following, we will provide a complete characterization of the asymptotic behavior of the single virus SIRIS model, for the two distinct scenarios of waning immunity ($\nu > 0$) and non-waning immunity ($\nu = 0$), respectively.

2.3. Results on the waning immunity scenario

We start by considering the asymptotic behavior of the single-virus SIRIS model in the case of waning immunity, i.e., when $\nu > 0$, and we establish the following result.

Theorem 1. *Assume $\nu > 0$. If $\lambda/\mu \leq 1$, then the solution of the single-virus model in Eq. (1) converges to the DFE; if $\lambda/\mu > 1$, then the solution of Eq. (1) converges to the unique EE $(\bar{x}, \bar{y})$ for any initial condition $x(0) > 0$, where*

$$\bar{x} = \frac{\alpha\lambda - \nu - \mu + \sqrt{(\alpha\lambda - \nu - \mu)^2 + 4\alpha\nu(\lambda - \mu)}}{2\alpha\lambda} \tag{4}$$

and

$$\bar{y} = \frac{\alpha\lambda - \nu - \mu + \sqrt{(\alpha\lambda - \nu - \mu)^2 + 4\alpha\nu(\lambda - \mu)}}{\alpha\lambda(\alpha\lambda + \nu - \mu + \sqrt{(\alpha\lambda - \nu - \mu)^2 + 4\alpha\nu(\lambda - \mu)})}. \tag{5}$$

Proof. Eq. (1) is a planar autonomous system, which means that no chaotic solutions are possible as a consequence of the Poincaré–Bendixson theorem—see, e.g., [31, 36] for more details. Moreover, it has a bounded domain (Proposition 1), and periodic orbits can be ruled out using the Bendixson–Dulac theorem [31], with Dulac function $\psi(x, y) = \frac{1}{x}$. In fact $\frac{\partial(\psi\dot{x})}{\partial x} + \frac{\partial(\psi\dot{y})}{\partial y} = -\lambda - \frac{\nu}{x} - \alpha\lambda < 0$.

Now, we compute the equilibria of the system by positing the right-hand-side of Eq. (1) equal to zero and we characterize their (local) stability via the Jacobian matrix:

$$J(x, y) = \begin{bmatrix} \lambda(1 - x - (1-\alpha)y) - \lambda x - \mu & -\lambda(1-\alpha)x \\ \mu - \alpha\lambda y & -\alpha\lambda x - \nu \end{bmatrix}. \tag{6}$$

From Eq. (1b), the DFE is the unique equilibrium on the boundary $x = 0$, which is unstable if $\lambda > \mu$ (from Eq. (6)), while it is locally asymptotically stable if $\lambda < \mu$. Convergence when $\lambda = \mu$ and global stability are consequences of the bound in Proposition 2.

Now we focus on EEs. From Eq. (1b), we obtain that at an equilibrium there holds $y = \mu x/(\alpha\lambda x + \nu)$, which, substituted into the equilibrium condition from Eq. (1a), yields the quadratic equation

$$f(x) = -\alpha\lambda^2 x^2 + (\alpha\lambda^2 - \lambda\nu - \lambda\mu)x + \nu(\lambda - \mu) = 0. \tag{7}$$

For $\lambda > \mu$, $f(0) > 0$, $f(1) < 0$, and $\lim_{x\to-\infty} f(x) = -\infty$. Hence, the two solutions of $f(x) = 0$ are such that one is negative and one lies in $[0, 1]$. The explicit computation of the second solution yields Eqs. (4)–(5), for which we check that $\bar{x} + \bar{y} \leq 1$. For $\lambda \leq \mu$, instead, a similar argument concludes that both solutions are nonpositive.

To prove that the unique EE (if it exists) is locally exponentially stable, we evaluate Eq. (6) at $(\bar{x}, \bar{y})$, obtaining

$$J(\bar{x}, \bar{y}) = \begin{bmatrix} -\lambda\bar{x} & -\lambda(1-\alpha)\bar{x} \\ \mu - \alpha\lambda\bar{y} & -\alpha\lambda\bar{x} - \nu \end{bmatrix}, \tag{8}$$

because at $(\bar{x}, \bar{y})$, Eq. (1a) yields $-\mu+\lambda(1-\bar{x}-(1-\alpha)\bar{y}) = 0$. Notice that $\mathrm{tr}(J(\bar{x}, \bar{y})) < 0$. We compute $\det(J(\bar{x}, \bar{y})) = \lambda^2\alpha(\bar{x})^2+\nu\lambda\bar{x}+\lambda(1-\alpha)\bar{x}(\mu-\alpha\lambda\bar{y}) = \lambda\bar{x}\mu(1-\alpha)+\lambda^2\bar{x}\alpha(\bar{x}+(1-\alpha)\bar{y}) + \nu\lambda\bar{x} > 0$. Hence, the eigenvalues of $J(\bar{x}, \bar{y})$ have negative real part, yielding local stability. Finally, the Poincaré–Bendixson theorem guarantees convergence to a fixed point [31], which is the unique EE. □

Remark 1. For $\nu > 0$, the conditions for stability of the DFE and the qualitative behavior when the DFE is unstable (i.e., convergence to a unique EE) coincide with those of a standard SIS model [3]. However, the exact value of the EE is indeed affected by immunity. Specifically, the epidemic prevalence in Eq. (4) is always smaller than that of the corresponding SIS model, which is equal to $1 - \mu/\lambda$. Moreover, from the monotonicity of $f(x)$ in Eq. (7) with respect to the model parameters, we observe that the EE $\bar{x}$ is monotonically increasing in α and decreasing in ν, in accord with intuition.

2.4. Results on the non-waning immunity scenario

We conclude this section by considering the special case in which immunity does not wane ($\nu = 0$). In this case, the behavior of the model is substantially different, as illustrated in the following result.

Theorem 2. *Assume $\nu = 0$. If $\lambda\alpha/\mu \leq 1$, then the single-virus model in Eq. (1) converges to the healthy manifold $\mathcal{H}$ and $x(t)$ is monotonically decreasing if $\lambda/\mu \leq 1$. If $\lambda\alpha/\mu > 1$, then the single-virus model in Eq. (1) converges to its unique EE $(\bar{x}, \bar{y}) = (1 - \frac{\mu}{\alpha\lambda}, \frac{\mu}{\alpha\lambda})$.*

Proof. When $\nu = 0$, Eq. (1) reduces to

$$\dot{x} = -\mu x + \lambda x(1 - x - (1-\alpha)y), \tag{9a}$$
$$\dot{y} = \mu x - \alpha\lambda xy. \tag{9b}$$

Similar to Theorem 1, the Poincaré–Bendixson theorem can be used to prove convergence to a fixed point [31]. From Eq. (9), we observe that the fixed points of the single-virus model are the entire healthy manifold (which includes the DFE), and the EE $(1 - \mu/\alpha\lambda, \mu/\alpha\lambda)$, which exists only if $\lambda\alpha > \mu$. The Jacobian in a generic point is

$$J(x, y) = \begin{bmatrix} \lambda - \mu - 2\lambda x - \lambda(1-\alpha)y & -\lambda(1-\alpha)x \\ \mu - \alpha\lambda y & -\alpha\lambda x \end{bmatrix}, \tag{10}$$

from which we observe that the EE is always stable when it exists. Moreover, if $\lambda\alpha > \mu$, then $\dot{x} > 0$ in the neighborhood of $x = 0$, implying that the system cannot converge to the healthy manifold from any point in the interior.

In contrast, if $\lambda \leq \mu$, we observe that $\dot{x} < 0$ in the entire domain. Hence, any trajectory converges to $\mathcal{H}$.

It is left to prove the behavior when $\mu < \lambda \leq \mu/\alpha$. For $\lambda \neq \mu/\alpha$, from Eq. (10), we observe that the healthy manifold can be split into two subsets: $\mathcal{H}_s = \{(x, y) : x = 0, y > \frac{\lambda-\mu}{\lambda(1-\alpha)}\} \subset \mathcal{H}$ and $\mathcal{H}_u = \mathcal{H} \setminus \mathcal{H}_s$. The line segment $\mathcal{H}_s$ is made of equilibrium points with a 0 eigenvalue (with eigenvector parallel to the line segment) and a negative eigenvalue with eigenvector orthogonal to the line. Hence, the points on this segment line are attractive in the direction orthogonal to the line segment 0. On the contrary, the line segment $\mathcal{H}_u$ is made of unstable equilibria. Hence, due to the absence of other fixed points, the system necessarily converges to the line segment $\mathcal{H}_s$ (which is part of the healthy manifold). Finally, when $\mu < \lambda \leq \mu/\alpha$, Eq. (9b) reads $\dot{y} = \mu x(1 - y)$, which implies that $y(t)$ is monotonically increasing until either $x = 0$ or $y = 1$ (where the latter implies $x = 0$), yielding convergence to $\mathcal{H}$. □

Remark 2. For $\nu = 0$, below the epidemic threshold $\lambda\alpha/\mu$, the disease is eradicated and the system converges to the healthy manifold, with part of the population recovered and part still susceptible. It is worth noticing that, while the exact proportion of the two compartments cannot be determined a priori since it may depend on the initial condition, we can lower-bound the fraction of recovered individuals as $\bar{y} > 1 - \frac{\mu}{\lambda(1-\alpha)}$, using the observations in the proof of Theorem 2. Above the epidemic threshold, instead, susceptible individuals eventually vanish, and the behavior of the model eventually coincides with a standard SIS model with contagion rate re-scaled by α.

3. General Bivirus SIRIS Model

When multiple competitive diseases are considered, natural immunity gains an additional dimensions of complexity. In fact, recovery from a specific virus may or may not grant protection against infection with a different virus —the former being the case of different orthopoxviruses [18, 19], the latter of influenza and RSVs [11]. On the top of this distinction between virus-specific and cross-immunity, each type of immunity can be partial, e.g., cross-immunity between different RSVs [17], and can wane in time, as for the strains of COVID-19 [20].

For these reasons, the development of compartmental models for multiple competitive viruses spreading in the same population is nontrivial, and requires specific care in the definition of the compartments for recovered individuals, and in the introduction of a suitable set of parameters to captures all the features discussed in the above. Before presenting such implementation, we briefly recall the standard bivirus SIS model [6] and we describe its emergent behavior. This will be key in the discussion of the impact of immunity on the epidemic process.

3.1. Bivirus SIS model

In the bivirus SIS model, three compartments are used to represent individuals who are susceptible (S), infected with virus 1 (I_1), and infected with virus 2 (I_2), respectively. We denote by $w(t) \in [0, 1]$ the fraction of population susceptible to the two viruses at time $t \geq 0$; and by $x_1(t)$ and $x_2(t)$ the fraction of the population infected with virus 1 and virus 2, respectively. Since $w(t) = 1 - x_1(t) - x_2(t)$, the dynamics of the bivirus SIS model is fully captured by the planar system of ODEs

$$\dot{x}_1 = -\mu_1 x_1 + \lambda_1(1 - x_1 - x_2)x_1 \tag{11a}$$
$$\dot{x}_2 = -\mu_2 x_2 + \lambda_2(1 - x_1 - x_2)x_2, \tag{11b}$$

with $\lambda_i > 0$ and $\mu_i > 0$ being the infection and recovery rates of virus i, respectively. The competitive nature of the two viruses is captured by the second term in Eq. (11), which couples the two equations. In fact, new infections with virus i occur with contagion rate $\lambda_i > 0$ when susceptible individuals (the fraction being $1 - x_1 - x_2$) come into contact with individuals infected with virus i (the fraction being x_i). In [6], Eq. (11) is analyzed, and the main results, reported in the following, depict a survival-of-the-fittest scenario: co-existence is only possible in the non-generic case of two equally infectious viruses.

Proposition 3 (From [6])**.** *If $\lambda_i/\mu_i \leq 1$ for both $i \in \{1, 2\}$, then Eq. (11) converges to the DFE $(\bar{x}_1, \bar{x}_2) = \mathbf{0}$. If $\lambda_i/\mu_i > \lambda_j/\mu_j$ and $\lambda_i/\mu_i > 1$, then Eq. (11) converges to the (unique) EE $(\bar{x}_1, \bar{x}_2)$, where $\bar{x}_i = 1-\mu_i/\lambda_i$ and $\bar{x}_j = 0$. Finally, if $\lambda_i/\mu_i = \lambda_j/\mu_j > 1$, then Eq. (11) converges an equilibrium on the line segment $(s, 1 - \mu_1/\lambda_1 - s)$, for all $s \in [0, 1 - \mu_1/\lambda_1]$.*

3.2. Bivirus SIRIS model

To capture the features arising from immunity, we build on a bivirus SIS model and we include two additional compartments accounting for individuals who have recovered from virus 1 and 2 (R_1 and R_2, respectively). Consequently, we add two variables to account for the fraction of the population recovered from virus 1 and 2 at time $t \geq 0$, denoted by $y_1(t)$ and $y_2(t)$, respectively. Similar to other compartmental models, we notice that $w(t) = 1 - x_1(t) - x_2(t) - y_1(t) - y_2(t)$. Hence, we can reduce the state space of the system to the four dimensional vector $(x_i(t), x_j(t), y_i(t), y_j(t)) \in \mathcal{D}$, where $\mathcal{D} := \{(x_i, x_j, y_i, y_j) \in [0, 1]^4 : x_1 + x_2 + y_1 + y_2 \leq 1\}$. Therefore, we propose the following four-dimensional system of ODEs to capture the disease spreading dynamics:

$$\begin{aligned}\dot{x}_1 = &-\mu_1 x_1 + (1 - x_1 - x_2 - (1 - \alpha_{11})y_1 \\ &- (1 - \alpha_{21})y_2)\lambda_1 x_1,\end{aligned} \tag{12a}$$
$$\dot{x}_2 = -\mu_2 x_2 + (1 - x_1 - x_2 - (1 - \alpha_{22})y_2$$

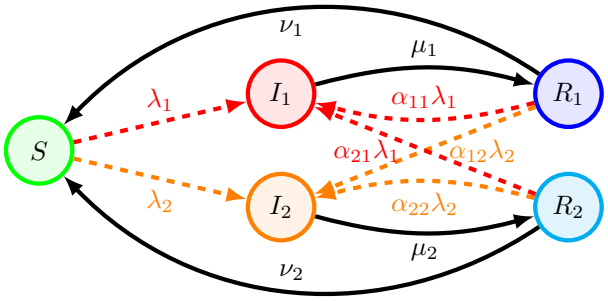

Figure 1: Schematic of the general model. Black solid arrows denote spontaneous transitions; red (orange) dashed arrows are transitions driven by interactions with individuals infected with virus 1 (2).

Table 1: Variables and parameters of the bivirus SIRIS model

symbol	meaning
$w(t)$	susceptible population at time t
$x_i(t)$	population infected with virus i at time t
$y_i(t)$	population recovered from virus i at time t
λ_i	contagion rate of virus i
μ_i	recovery rate from virus i
ν_i	rate of waning immunity from virus i
α_{ii}	virus-specific immunity against virus i
α_{ij}	cross immunity against virus j

$$-(1-\alpha_{12})y_1)\lambda_2 x_2, \tag{12b}$$

$$\dot{y}_1 = \mu_1 x_1 - \nu_1 y_1 - \alpha_{11}\lambda_1 y_1 x_1 - \alpha_{12}\lambda_2 y_1 x_2, \tag{12c}$$

$$\dot{y}_2 = \mu_2 x_2 - \nu_2 y_2 - \alpha_{21}\lambda_1 y_2 x_1 - \alpha_{22}\lambda_2 y_2 x_2. \tag{12d}$$

Similar to the bivirus SIS model in Section 3.1, the parameters λ_i and μ_i captures the infection and recovery rate of virus i, respectively. However, once recovered, an individual acquires partial immunity against the two viruses. Specifically, for each virus i, we introduce two parameters $\alpha_{ii} \in [0,1]$ and $\alpha_{ij} \in [0,1]$, which captures virus-specific immunity and cross immunity due to recovery from virus i, respectively ($\alpha_{ii} = 1$ and $\alpha_{ij} = 1$ models absence of virus-specific and cross immunity, respectively; $\alpha_{ii} = 0$ and $\alpha_{ij} = 0$ model perfect virus-specific and cross immunity, respectively). Such parameters affect the contagion rate of the corresponding viruses as multiplicative factors, similar to the single-virus SIRIS model illustrated in Section 2. Natural immunity due to infection from virus i wanes at a rate $\nu_i \geq 0$, and the individual becomes susceptible again. Hence, for each virus i, the characteristics of immunity in terms of level of virus-specific protection, level of cross-protection, and duration are captured by the three parameters α_{ii}, α_{ij}, and ν_i, respectively. The model is illustrated in Fig. 1 and all variables and parameters are summarized in Table 1. We introduce some terminology.

Definition 2. *The healthy manifold is defined as* $\mathcal{H} := \{(x_1, x_2, y_1, y_2) \in \mathcal{D} : x_1 = x_2 = 0\}$, *and the DFE as* $(x_1, x_2, y_1, y_2) = \mathbf{0}$. *Given a fixed point of Eq. (12),* $(\bar{x}_i, \bar{x}_j, \bar{y}_i, \bar{y}_j) \in \mathcal{D}$, *the point is an EE if* $\bar{x}_1 + \bar{x}_2 > 0$. *Specifically, the fixed point is a boundary (endemic) equilibrium (BEE) if* $\bar{x}_1 > 0$ *and* $\bar{x}_2 = 0$ *or* $\bar{x}_1 = 0$ *and* $\bar{x}_2 > 0$, *and it is a co-existence (endemic) equilibrium (CEE) if both* $\bar{x}_1 > 0$ *and* $\bar{x}_2 > 0$.

4. Results on the General Bivirus SIRIS Model

In the following, after reporting a result that guarantees the well-posedness of the bivirus SIRIS model in Eq. (12) in terms of the invariance of the domain and of the healthy manifold, we prove a general result to characterize the stability of the DFE in the scenario of waning immunity.

Proposition 4 (Proposition 3 from [29])**.** *The domain* $\mathcal{D}$ *and the healthy manifold* $\mathcal{H}$ *are positively invariant for Eq. (12). Moreover, if* $(x_1(0), x_2(0), y_1(0), y_2(0)) \in \mathcal{H}$ *and* $\nu_1, \nu_2 > 0$, *then* $\lim_{t\to\infty}(x_1(t), x_2(t), y_1(t), y_2(t)) = \mathbf{0}$.

Theorem 3. *Let* $\nu_1 > 0$ *and* $\nu_2 > 0$. *Then, the DFE is globally asymptotically stable for Eq. (12) if and only if (iff)* $\lambda_i \leq \mu_i$, *for* $i \in \{1,2\}$ *(with exponential stability if both inequalities are strict), and it is unstable otherwise.*

Proof. For the sufficiency, we verify that, for $\lambda_i \leq \mu_i$, the DFE is globally asymptotically stable. In fact, for $\lambda_i < \mu_i$, from Eqs. (12a)–(12b), we can bound $\dot{x}_i \leq -(\mu_i - \lambda)x_i$. Using Gronwall's inequality [30], we bound $x_i(t) \leq x(0)\exp\{-(\mu_i - \lambda_i)t\}$. Similar, for $\lambda_i = \mu_i$, we bound $\dot{x}_i \leq -\mu_i x_i^2$, yielding $x_i(t) \leq \frac{x(0)}{\mu_i t+1}$. In both cases it holds $x_i(t) \to 0$, but convergence is exponentially fast only in the first case. Then, using Eq. (12c) and Eq. (12d), for $i, j \in \{1,2\}$ and $i \neq j$, there holds

$$\dot{y}_i = -\nu_i y_i + \mu_i x_i - \lambda_j x_j y_i = -\nu_i y_i + \omega_i(t), \tag{13}$$

with $\omega_i(t)$ being an input signal that decays to zero, whereas Eq. (13) with no input would converge to 0 exponentially fast (being $\nu_i > 0$). Evidently, $\lim_{t\to\infty} y_i(t) = 0$ for all $i = 1, 2$, which yields the first part of the claim.

For necessity, we evaluate the Jacobian of the right side of Eq. (12) at the DFE, obtaining a lower triangular matrix with diagonal entries equal to $\lambda_1 - \mu_1$, $\lambda_2 - \mu_2$, $-\nu_1$, and $-\nu_2$, concluding that the DFE is unstable if at least one of the two ratios $\lambda_i/\mu_i > 1$, yielding the claim. □

While a general characterization of the EEs is a challenging problem, we can explicitly compute the BEEs and prove that CEEs (if present) are finite in number, for almost any value of the parameters.

Proposition 5. *Let* $\nu_1 > 0$ *and* $\nu_2 > 0$. *Then, the bivirus SIRIS model in Eq. (12) has at most two BEEs, of the form* $(\bar{x}_1, \bar{x}_2, \bar{y}_1, \bar{y}_2)$, *where* $\bar{x}_j = \bar{y}_j = 0$,

$$\bar{x}_i = \frac{\alpha_{ii}\lambda_i - \nu_i - \mu_i + \sqrt{(\alpha_{ii}\lambda_i - \nu_i - \mu_i)^2 + 4\alpha_{ii}\nu_i(\lambda_i - \mu_i)}}{2\alpha_{ii}\lambda_i} \tag{14}$$

and

$$\bar{y}_i = \frac{\mu_i \bar{x}_i}{\nu_i + \alpha_{ii}\lambda x_i}, \tag{15}$$

which exists iff $\lambda_i > \mu_i$*, for* $i \in \{1, 2\}$ *and* $j \neq i$*.*

Proof. We derive the equilibrium conditions by equating the right-hand side of Eq. (12) to 0. Without any loss in generality, we consider the boundary $\bar{x}_i = 0$. From Eq. (12c), we observe that for an equilibrium on the boundary $\bar{x}_1 = 0$ to exist, there necessarily holds $\bar{y}_1 = 0$. By substituting these conditions into Eq. (12d), we obtain

$$\bar{y}_2 = \frac{\mu_2 x_2}{\nu_2 + \alpha_{22}\lambda x_2} \tag{16}$$

By replacing $\bar{x}_1 = \bar{y}_1 = 0$ and Eq. (16) into the equilibrium condition from Eq. (12b), we obtain the equilibrium condition for a single-virus SIRIS model with $\lambda = \lambda_2$, $\mu = \mu_2$, $\nu = \nu_2$, and $\alpha = \alpha_{22}$, studied in Theorem 1, which yields the claim. □

Proposition 6. *The bivirus SIRIS model in Eq. (12) has a finite number of CEEs (possibly none), which are nondegenerate, for almost all the parameter values.*

Proof. Let us consider a generic coexistence equilibrium (x_1, x_2, y_1, y_2), with $x_1 \neq 0, x_2 \neq 0$. Let us denote the vector field in Eq. (12) by F, by $\boldsymbol{p} = [\mu_1, \mu_2, \nu_1, \nu_2, \lambda_1, \lambda_2]^\top$ a vector of parameters and $\boldsymbol{v} = [x_1, x_2, y_1, y_2]^\top$ the state vector that gathers the four variables of the system.

Let $g_1 := [1 - x_1 - x_2 - (1 - \alpha_{11})y_1 - (1 - \alpha_{21})y_2]x_1$ and $g_2 := [1 - x_1 - x_2 - (1 - \alpha_{12})y_1 - (1 - \alpha_{22})y_2]x_2$, then we can consider the vector field F as function also of the parameter vector $\boldsymbol{p}$, and write the Jacobian of $F(\boldsymbol{v}, \boldsymbol{p})$ with respect to the parameters $\boldsymbol{p}$:

$$\boldsymbol{J}_{\boldsymbol{p}} = \begin{bmatrix} -x_1 & 0 & 0 & 0 & g_1 & 0 \\ 0 & -x_2 & 0 & 0 & 0 & g_2 \\ x_1 & 0 & -y_1 & 0 & -\alpha_{11}y_1x_1 & -\alpha_{12}y_1x_2 \\ 0 & x_2 & 0 & -y_2 & -\alpha_{21}y_2x_1 & -\alpha_{22}y_2x_2 \end{bmatrix}. \tag{17}$$

From Eq. (12c), we observe that at a co-existence equilibrium, it necessarily holds that $y_1 \neq 0$ and $y_2 \neq 0$. Hence, it is clear from considering the first four columns that $\boldsymbol{J}_{\boldsymbol{p}}$ has rank 4. Further, the equilibrium equations give $\mu_i = g_i\lambda_i$, which shows that the g_i are both nonzero.

Let $\mathcal{V}$ and $\mathcal{P}$ denote the associated open sets of allowed $\boldsymbol{v}$ and $\boldsymbol{p}$, with the openness guaranteeing they are manifolds. Let $\mathcal{W}$ denote the manifold that is the image of $\mathcal{V} \times \mathcal{P}$ under Eq. (12), thus $\mathcal{W} = \{\boldsymbol{w} : \boldsymbol{w} = F(\boldsymbol{v}, \boldsymbol{p})\}$. Let $\mathcal{Z} := \{\boldsymbol{0}\}$, where $\boldsymbol{0}$ is the 4-dimensional all-zero vector. The calculation above demonstrates that the Jacobian $\boldsymbol{J}_{\boldsymbol{p}}$ in Eq. (17) has rank 4 at any point in $\mathcal{V} \times \mathcal{P}$ which maps to $\mathcal{Z}$, so *a fortiori* the Jacobian $\boldsymbol{J}_{\boldsymbol{v},\boldsymbol{p}}$ (which is obtained by adding columns to Eq. (17)) has rank 4 at any such point. Hence $F : \mathcal{V} \times \mathcal{P} \to \mathcal{W}$ is transversal to $\mathcal{Z}$, and by the parametric transversality theorem (see [32, p.145] and [33, p. 68]), for almost all particular $\bar{\boldsymbol{p}} \in \mathcal{P}$, i.e., excluding a set of zero measure, the Jacobian $\boldsymbol{J}_{\boldsymbol{v}}$ associated with the mapping $F_{\bar{\boldsymbol{p}}} : \mathcal{V} \to \mathcal{W}$, with $F_{\bar{p}}(\boldsymbol{v}) = f(\boldsymbol{v}, \bar{\boldsymbol{p}})$ will have full row rank at any zero, i.e., for $\boldsymbol{v}$ such that $F_{\bar{\boldsymbol{p}}}(v) = \boldsymbol{0}$. Equivalently, for almost all $\bar{\boldsymbol{p}}$, a zero of $F_{\bar{p}}$ gives rise to a nonsingular Jacobian or the zero is nondegenerate (and consequently isolated). The bounded nature of $\mathcal{D}$ implies that there can only be a finite number of equilibria. □

Remark 3. Note that the argument used in the proof of Proposition 6 does not take into account the values of the parameters α_{ij}. Hence, a corollary of Proposition 6 is that, for any fixed α_{11}, α_{22}, α_{12}, and α_{21}, the bivirus SIRIS model has a finite number of nondegenerate CEEs for almost all the parameter values.

We report here an intuitive but important result for the case $\nu_1 = \nu_2 = 0$, which models situations in which, following infection, some permanent level of immunity remains. In this scenario, it is intuitive that, if the disease becomes endemic, then the pool of susceptible individuals goes to zero: once a person has had a virus, they can never return to the susceptible state. The following result from [29] provides theoretical guarantees to such an intuition.

Proposition 7 (Proposition 4 from [29])**.** *If* $\nu_1 = \nu_2 = 0$*, then either Eq. (12) converges to* $\mathcal{H}$ *or* $\lim_{t\to\infty} w(t) = 0$*.*

Above, consideration is given as to what happens in the non-waning immunity scenario, when both $\nu_i = 0$. We now ask what happens in the opposite scenario of fast-waning immunity, i.e., when $\nu_i \to \infty$. Intuition is that any individuals who are (temporarily) immune will lose that immunity arbitrarily fast, implying that there cannot be a nonzero endemic value possible for y_i. If both ν_i go to infinity, the system should then be indistinguishable from the bivirus SIS model in Eq. (11). The following result formalizes this intuition.

Proposition 8. *Let* $\nu_i \to \infty$ *for* $i = 1$ *or* $i = 2$ *(both possibilities being permitted). Then, Eq. (12) is such that* $y_i(t) \to 0$ *for any* $t > 0$*. Moreover, if both* $\nu_1, \nu_2 \to \infty$*, then the ODEs for* x_1 *and* x_2 *with* $t > 0$ *become identical to those for the bivirus SIS model in Eq. (11).*

Proof. Suppose without loss of generality that $i = 1$. Then

$$\begin{aligned} \dot{y}_1 &= \mu_1 x_1 - (\nu_1 + \alpha_{11}\lambda_1 x_1 + \alpha_{12}\lambda_2 x_2)y_1 \\ &= u(t) - \big(a(t) + \nu_1\big)y_1 \end{aligned} \tag{18}$$

where $u(t) = \mu_1 x_1$ is bounded and nonnegative, $a(t) = \alpha_{11}\lambda_1 x_1 + \alpha_{12}\lambda_2 x_2$ is bounded and nonnegative, and importantly, the derivative of $u(t)$ is bounded, the claim being easily checked. A conventional singular perturbation argument appears awkward to apply, and we use a 'first principles' style of argument.

The solution of Eq. (18) is the sum of a zero input component, call it $\tilde{y}(t)$, arising from the initial condition $y_1(0)$, and a zero-initial-state component, call it $\hat{y}(t)$, arising from the "input" $u(t)$. The zero-input component is the solution

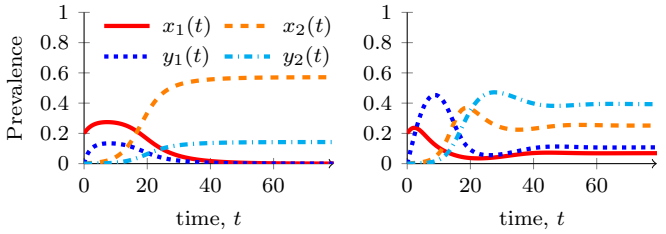

(a) $\nu_1 = \nu_2 = 0.8$ (b) $\nu_1 = \nu_2 = 0.08$

Figure 2: Simulations of the bivirus SIRIS model with $\lambda_1 = \lambda_2 = 0.7$, $\mu_1 = 0.4$, $\mu_2 = 0.2$, $\alpha_{11} = \alpha_{22} = 0$, and $\alpha_{12} = \alpha_{21} = 1$.

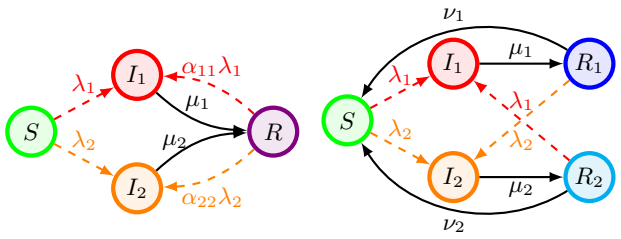

(a) Model I (b) Model II

Figure 3: Schematics of the two specializations of the SIRIS model.

of $\frac{d}{dt}\tilde{y}_1 = -(a(t)+\nu_1)\tilde{y}_1$, i.e., $\tilde{y}(t) = y_1(0)\exp\{\int_0^t(-a(s)-\nu_1)ds)\}$, and it clearly goes to zero at any nonzero t when $\nu_1 \to \infty$. For the zero-initial-state component, there holds $\hat{y}_1(t) = \int_0^t \exp\{\int_0^s(-a(\sigma)-\nu_1)d\sigma\}u(t-s)ds$. Since $u(t) > 0$ for all t, the integral is nonnegative and in fact $0 \leq \hat{y}^1(t) \leq \int_0^t e^{-\nu_1 s}u(t-s)ds = -\frac{1}{\nu}(e^{-\nu_1 t}u(0) - u(t)) + \frac{1}{\nu}\int_0^t e^{-\nu_1 s}\frac{d}{ds}u(t-s) \leq -\frac{1}{\nu}(e^{-\nu_1 t}u(0)-u(t))+\nu^{-2}M$, where M is an upper bound on $|\dot{u}(t)|$. Letting ν_1 go to infinity establishes the lemma claim for $y_1(t)$. It is immediate that if for $t > 0$ one replaces $y_1(t)$ and $y_2(t)$ by zero in the differential equations for x_1 and x_2 one recovers Eq. (11). □

While the general bivirus SIRIS model is amenable to some analytical treatment, such as characterizing the stability of the DFE (see Theorem 3) and investigating relevant limit cases (see, e.g., Proposition 8), its general study is challenging, being Eq. (12) made of four independent nonlinear equations regulated by 10 parameters. Nonetheless, numerical simulations reported in Fig. 2 illustrate a wide range of emergent behaviors, which include not only survival-of-the-fittest scenarios (see Fig. 2a), similar to what happens in the standard SIS model, but also stable co-existence of the two viruses for generic values of the parameters (see Fig. 2b), which cannot emerge in the standard SIS model [6].

To provide analytical evidence to such observations, in the rest of this paper we focus on two specializations of the model, which are amenable to analytical treatment. First, we derive a specialized model that focuses on the role of partial immunity, neglecting waning immunity and the (possible) differences between virus-specific and cross immunity. This study aims to provide some insight into diseases with multiple strain, where recovery from one strain provides a certain level of immunity against the same strain and other strains, but not complete immunity. This is the case, for instance, for COVID-19 [20–22]. Second, we simplify our general model to study the role of virus-specific waning immunity. This study aim to provide insights into diseases such as seasonal flu and cold [10, 11], which despite being competitive, are often observed stably co-existing in the population [16]. Each of the two specializations obtained is characterized by only six parameters: four are common and are associated with the characteristics of the two viruses: λ_1, λ_1, μ_1, μ_2; two are specific to the particular phenomenon under analysis.

5. Model I: Partial immunity

In this first specialization, we focus on understanding the effect of partial immunity. Thus, we assume that after recovery from either of the two viruses, an individual acquires a certain level of immunity against both viruses, which may be different between the two viruses, but with no distinction between virus-specific and cross immunity. Moreover, we neglect waning immunity. To some extent, these assumptions may capture scenarios with multiple strains of a virus during an epidemic outbreak, where immunity waning occurs on a much slower time-scale than the competition between different strains. This was the case, e.g., in the emergence of the Omicron variant of COVID-19 in late 2021 [13].

Briefly, our assumptions can be summarized in the following set of conditions on the model parameters.

Assumption 1. *Let $\nu_1 = \nu_2 = 0$, $\alpha_{21} = \alpha_{11}$, $\alpha_{12} = \alpha_{22}$.*

Intuitively, since virus-specific immunity and cross immunity are assumed to have the same effect, there is no need to define two distinct variables for the recovered compartments. Hence, if we define $y = y_1 + y_2$, we can reduce the dynamics in Eq. (12) under Assumption 1 to the following three dimensional system:

$$\dot{x}_1 = -\mu_1 x_1 + (1 - x_1 - x_2 - (1-\alpha_{11})y)\lambda_1 x_1, \quad (19a)$$
$$\dot{x}_2 = -\mu_2 x_2 + (1 - x_1 - x_2 - (1-\alpha_{22})y)\lambda_2 x_2, \quad (19b)$$
$$\dot{y} = \mu_1 x_1 + \mu_2 x_2 - \alpha_{11}\lambda_1 x_1 y - \alpha_{22}\lambda_2 x_2 y, \quad (19c)$$

as illustrated in Fig. 3a. The model is fully determined by six parameters: λ_1, λ_2, μ_1, μ_2, α_{11}, and α_{22}.

The analysis of the partial immunity model is two-fold. First, we study its transient behavior, establishing bounds on its evolution in terms of simpler bivirus SIS models, extending the bounding arguments used in Proposition 2. Second, using Proposition 7, we characterize the asymptotic behavior of the bivirus model.

5.1. Results on the transient behavior

The earlier results for a single virus model with immunity showed how two SIS models can be found whose

solutions provide upper and lower bounds for a specified SIRIS model. This motivates the following material, where similar bounds are provided for the bivirus case. In particular, we start by presenting the following technical lemma, whose proof is reported in Appendix A.

Lemma 1. *Consider the Partial Immunity Model in Eq. (19) with initial conditions satisfying* $x_1(0) \geq 0, x_2(0) \geq 0, x_1(0) + x_2(0) \leq 1$. *Then there hold*

$$\dot{x}_1 \geq -\mu_1 x_1 + \lambda_1 \alpha_{11}(1 - x_1 - x_2)x_1 \tag{20a}$$
$$\dot{x}_2 \leq -\mu_2 x_2 + \lambda_2(1 - x_1 - x_2)x_2 \tag{20b}$$

and also

$$\dot{x}_1 \leq -\mu_1 x_1 + \lambda_1(1 - x_1 - x_2)x_1 \tag{21a}$$
$$\dot{x}_2 \geq -\mu_2 x_2 + \lambda_2 \alpha_{22}(1 - x_1 - x_2)x_2 \tag{21b}$$

Moreover, if $\alpha_{11} \neq 1, \alpha_{22} \neq 1$, $x_1(0) > 0, x_2(0) > 0$ *and* $w(0) = 1 - x_1 - x_2 - y > 0$, *then the four inequalities are strict for all* $t > 0$.

The inequalities above are the key to obtaining SIS systems whose trajectories bound those of the SIRIS system. The technique for doing this is to use draw on results for positive systems, see [37].

Proposition 9. *Consider the Partial Immunity Model in Eq. (19) with initial conditions satisfying* $x_1(0) \geq 0, x_2(0) \geq 0, x_1(0) + x_2(0) \leq 1$. *Consider the following two bivirus SIS systems:*

$$\dot{u}_1 = -\mu_1 u_1 + \lambda_1 \alpha_{11}(1 - u_1 - u_2)u_1 \tag{22a}$$
$$\dot{u}_2 = -\mu_2 u_2 + \lambda_2(1 - u_1 - u_2)u_2 \tag{22b}$$

and

$$\dot{v}_1 = -\mu_1 v_1 + \lambda_1(1 - v_1 - v_2)v_1 \tag{23a}$$
$$\dot{v}_2 = -\mu_2 v_2 + \lambda_2 \alpha_{22}(1 - v_1 - v_2)v_2 \tag{23b}$$

Suppose that $x_1(0) = u_1(0) = v_1(0), x_2(0) = u_2(0) = v_2(0)$. *Then for all* t, *there holds*

$$v_1(t) \geq x_1(t) \geq u_1(t), \quad v_2(t) \leq x_2(t) \leq u_2(t). \tag{24}$$

If $\alpha_{11} \neq 1, \alpha_{22} \neq 1$, *and* $x_1(0), x_2(0)$ *and* $w(0)$ *are all positive, then the inequalities are strict for all* t.

Proof. We shall prove only the inequalities in Eq. (22); the inequalities in Eq. (23), being obtained by the same procedure. To enable applicability of the comparison theorem for differential equations [37], we need to introduce new variables $\tilde{x}_2(t) = -x_2(t)$ and $\tilde{u}_2(t) = -u(t)$, so that the differential inequalities are all in the same direction. Using Eq. (20a), we see that $\dot{x}_1 - \dot{u}_1 \geq -\mu_1 x_1 + \lambda_1 \alpha_{11}(1 - x_1 + \tilde{x}_2)x_1 + \mu_1 u_1 - \lambda_1 \alpha_{11}[1 - u_1 + \tilde{u}_2]u_1 = [-\mu_1 + \lambda_1 \alpha_{11}(1 - x_1 - u_1)](x_1 - u_1) + \lambda_1 \alpha_{11}(\tilde{x}_2 x_1 - \tilde{u}_2 u_1)]$. Now since $\tilde{x}_2 x_1 - \tilde{u}_2 u_1 = \tilde{x}_2(x_1 - u_1) + (\tilde{x}_2 - \tilde{u}_2)u_1$, we have that $\dot{x}_1 - \dot{u}_1 \geq [-\mu_1 + \lambda_1 \alpha_{11}(1 - x_1 - u_1 + \tilde{x}_2)](x_1 - u_1) + \lambda_1 \alpha_{11} u_1(\tilde{x}_2 - \tilde{u}_2)$. A similar argument yields $\dot{\tilde{x}}_2 - \dot{\tilde{u}}_2 \geq -\lambda_2 \tilde{u}_2(x_1 - u_1) + [-\mu_2 + \lambda_2(1 + \tilde{x}_2 + \tilde{u}_2 - x_1)](\tilde{x}_2 - \tilde{u}_2)$.

Let us set $\alpha = x_1 - u_1, \beta = \tilde{x}_2 - \tilde{u}_2$. Then there are time functions $g_{ij}(t)$ such that $\dot{\alpha} \geq g_{11}(t)\alpha + g_{12}(t)\beta$ and $\dot{\beta} \geq g_{21}(t)\alpha + g_{22}(t)\beta$, with strict inequality at time t in case $\alpha_{11} \neq 1, \alpha_{22} \neq 1$ and $x_1(0), x_2(0)1 - x_1(0) - x_2(0) - y(0)$ all positive. Moreover, the functions g_{12} and g_{21} are nonnegative for all $t \geq 0$ (and it is irrelevant that they can be expressed in terms of some of the variables of interest). Since also $\alpha(0) = 0, \beta(0) = 0$, there holds $\alpha(t) \geq 0, \beta(t) \geq 0$ for all $t \geq 0$, (with strict inequality under the stated conditions), i.e., the result follows [37, Lemma VIII.1]. □

5.2. Results on the asymptotic behavior

Here, we will discuss the asymptotic behavior of the Partial Immunity Model in Eq. (19). Specifically, we start by reporting a result from [29], which establish conditions under which EEs exist and they are (almost) globally asymptotically stable, with the exception of a set of non-generic parameter values.

Proposition 10 (Proposition 7 from [29])**.** *If* $\frac{\alpha_{11}\lambda_1}{\mu_1} \neq \frac{\alpha_{22}\lambda_2}{\mu_2}$, *Eq. (19) admits at most two EEs, coinciding with the BEEs:*

$$(x_1, x_2, y) = \left(\frac{\alpha_{11}\lambda_1 - \mu_1}{\alpha_{11}\lambda_1}, 0, \frac{\mu_1}{\alpha_{11}\lambda_1}\right), \tag{25a}$$
$$(x_1, x_2, y) = \left(0, \frac{\alpha_{22}\lambda_2 - \mu_2}{\alpha_{22}\lambda_2}, \frac{\mu_2}{\alpha_{22}\lambda_2}\right), \tag{25b}$$

which exist iff $\alpha_{11}\lambda_1 > \mu_1$ *and* $\alpha_{22}\lambda_2 > \mu_2$, *respectively. Eq. (25a) is locally asymptotically stable iff* $\frac{\alpha_{11}\lambda_1}{\mu_1} > \frac{\alpha_{22}\lambda_2}{\mu_2}$; *while Eq. (25b) is locally asymptotically stable iff* $\frac{\alpha_{11}\lambda_1}{\mu_1} < \frac{\alpha_{22}\lambda_2}{\mu_2}$. *In each case, the locally asymptotically stable BEE is globally stable for all initial conditions in the interior of* $\{(x_1, x_2, y) \in [0, 1]^3 : x_1 + x_2 + y \leq 1\}$.

Proposition 10 complete characterizes the behavior of the epidemic model when at least one of the viruses is sufficiently infectious, that is, $\alpha_{ii}\lambda_i > \mu_i$ for at least one $i \in \{1, 2\}$, and when $\frac{\alpha_{11}\lambda_1}{\mu_1} \neq \frac{\alpha_{22}\lambda_2}{\mu_2}$. In the following, we investigate the nongeneric case $\frac{\alpha_{11}\lambda_1}{\mu_1} = \frac{\alpha_{22}\lambda_2}{\mu_2}$, in which, as proved below, a line segment of equilibria is present.

Proposition 11. *If* $\alpha_{11}\lambda_1/\mu_1 = \alpha_{22}\lambda_2/\mu_2 > 1$, *Eq. (19) admits the line segment of equilibria* $(0, x_1, 1 - \frac{\mu_1}{\alpha_{11}\lambda_1} - x_1, \frac{\mu_1}{\alpha_{11}\lambda_1})$, *with* $x_1 \in [0, \frac{\mu_1}{\alpha_{11}\lambda_1}]$. *When it exists, such a segment is always globally attractive from any initial condition in the interior.*

Proof. If $\alpha_{11}\lambda_1/\mu_1 = \alpha_{22}\lambda_2/\mu_2$, then the equilibrium conditions for Eq. (19a) and Eq. (19a) coincide and are equal to $x_1 + x_2 = \frac{\alpha_{11}\lambda_1 - \mu_1}{\alpha_{11}\lambda_1}$, which yields the line segment of equilibria. If we evaluate the Jacobian of Eq. (19) in the generic point of the line segment and we compute its eigenvalues, we obtain that one is equal to 0 (with eigenvector parallel to the line segment), while the other two are

always negative and equal to $-(\alpha_{11}\lambda_1 x_1 + \alpha_{22}\lambda_2 x_2)$ and $-(\lambda_1 x_1 + \lambda_2 x_2)$, yielding local stability in the directions orthogonal to the line segment. Global convergence is finally proved similarly to Proposition 10, using the argument that $w(t)$ converges exponentially fast to 0, reducing the system to a standard bivirus SIS model with an exponentially vanishing additive term, and then using again the theoretical results from [6, 31, 38]. □

The results above consider scenarios in which at least one of the viruses is sufficiently infectious so that it remains endemic in the population, that is, when at least one of the ratios $\frac{\alpha_{ii}\lambda_i}{\mu_i} > 1$. Now, we study the opposite scenario, i.e., when both $\frac{\alpha_{11}\lambda_1}{\mu_1} \leq 1$ and $\frac{\alpha_{22}\lambda_2}{\mu_2} \leq 1$, which yields eradication of the disease, as summarized in the following, with proof reported in Appendix B.

Proposition 12. *If $\alpha_{ii}\lambda_i \leq \mu_i$ for both $i \in \{1,2\}$, Eq. (19) possesses a line segment of equilibria defined by $x_1 = x_2 = 0, y \in [0,1]$. If $\alpha_{ii}\lambda_i < \mu_i$ for both $i \in \{1,2\}$, an equilibrium on this line is (locally) attractive in directions orthogonal to the line iff*

$$y \in \left(\max\left[\frac{\lambda_1 - \mu_1}{\lambda_1(1-\alpha_{11})}, \frac{\lambda_2 - \mu_2}{\lambda_2(1-\alpha_{22})}\right], 1\right], \qquad (26)$$

which is never empty. If $\alpha_{11}\lambda_1 = \mu_1$ or $\alpha_{22}\lambda_2 = \mu_2$, then the only attractive point on this line is $(0,0,1)$. Moreover, Eq. (19) always converges to the healthy manifold $\mathcal{H}$.

We now consolidate all our findings from Propositions 10–12 in a theorem, which is the main result of this section and provides a complete characterization of the asymptotic behavior of Eq. (19).

Theorem 4. *Consider the Partial Immunity Model in Eq. (19). Then, the following holds true.*

1. *If $\lambda_i\alpha_{ii}/\mu_i \leq 1$ for both $i \in \{1,2\}$, Eq. (19) converges to the healthy manifold $\mathcal{H}$ for any initial condition. Specifically, it converges to an equilibrium point of the form $(0,0,y)$, with y that satisfies Eq. (26).*

2. *If $\lambda_i\alpha_{ii}/\mu_i > 1$ and $\lambda_i\alpha_{ii}/\mu_i > \lambda_j\alpha_{jj}/\mu_j$, for $j \neq i \in \{1,2\}$, then Eq. (19) converges to the BEE with $\bar{x}_i = 1 - \frac{\mu_i}{\alpha_{ii}\lambda_i}$, $\bar{x}_j = 0$, and $\bar{y} = \frac{\mu_i}{\alpha_{ii}\lambda_i}$, for any initial condition in the interior of the domain.*

3. *If $\lambda_1\alpha_{11}/\mu_1 = \lambda_2\alpha_{22}/\mu_2 > 1$, then Eq. (19) converges to the line segment of equilibria $(x_1, 1 - \frac{\mu_1}{\alpha_{11}\lambda_1} - x_1, \frac{\mu_1}{\alpha_1\lambda_1})$, with $x_1 \in [0, \frac{\mu_1}{\alpha_{11}\lambda_1}]$ for any initial condition in the interior of the domain.*

The simulations in Fig. 4 illustrates the findings in Theorem 4. In particular, we consider two viruses with $\lambda_1/\mu_1 = \lambda_2/\mu_2 > 1$, and we observe the behavior when changing α_{11} and α_{22}. As predicted by item 1, when both α_{ii} are small so that $\alpha_{ii}\lambda_i/\mu_i < 1$, the disease is eradicated and the system converges to an equilibrium on the healthy manifold (as reported in Fig. 4a). Figs. 4b and 4c show a survival-of-the-fittest scenario, where the virus with largest $\alpha_{ii}\lambda_i/\mu_i$ remains endemic. Interestingly, in Fig. 4c, where both viruses have $\alpha_{ii}\lambda_i/\mu_i > 1$, after an initial outbreak of virus 1 (which has larger value of λ_i), virus 2 becomes dominant, as predicted by item 2. Finally, in Fig. 4d, we illustrate the scenario predicted by item 3, where the system converges to a point on the line of EEs, with co-existence of the two viruses.

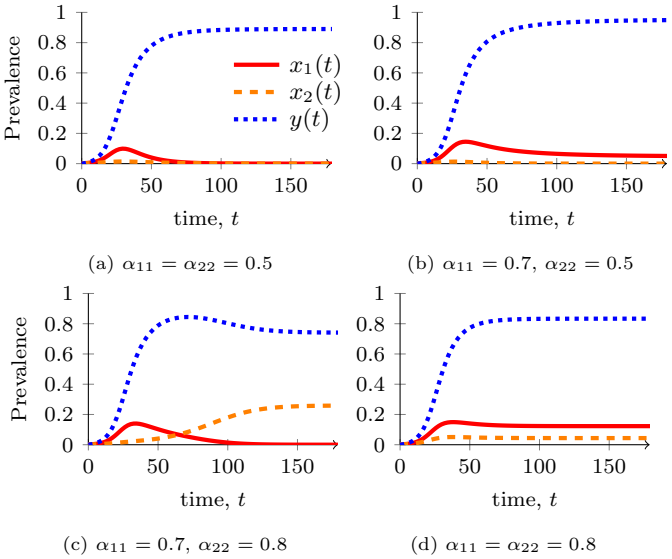

(a) $\alpha_{11} = \alpha_{22} = 0.5$ (b) $\alpha_{11} = 0.7$, $\alpha_{22} = 0.5$

(c) $\alpha_{11} = 0.7$, $\alpha_{22} = 0.8$ (d) $\alpha_{11} = \alpha_{22} = 0.8$

Figure 4: Simulations of Model I with $\lambda_1 = 0.6$, $\lambda_2 = 0.45$, $\mu_1 = 0.4$, $\mu_2 = 0.3$, and different values of α_{11} and α_{22}.

Remark 4. The emergent behavior of the Partial Immunity model in Eq. (19) resembles that of a bivirus SIS model presented in Section 3.1, wherein (except for a non-generic set of parameter values) we observe either eradication of both diseases or survival-of-the-fittest virus. However, unlike the standard SIS model, the fitter virus is not the one with largest basic reproduction number (i.e., λ_i/μ_i), but such a value is modulated by the (potentially different) level of protection against the two viruses acquired after recovery.

6. Model II: Waning Virus-specific Immunity

We consider now a second specialization of the model, in which we focus on unveiling the effects of simultaneous waning and virus-specific immunity. To this aim, we assume that after recovery from either of the two viruses, an individual acquires full (but waning) immunity only against that virus, while no immunity is acquired against the other virus. For instance, this is the case of the influenza A virus and rhinovirus (which cause flu and cold, respectively), for which no (or very limited) cross-immunity has been observed [10].

Assumption 2. *Let $\alpha_{11} = \alpha_{22} = 0$, $\alpha_{12} = \alpha_{21} = 1$, $\nu_1 > 0$, and $\nu_2 > 0$.*

Under Assumption 2, Eq. (12) reduces to

$$\dot{x}_1 = -\mu_1 x_1 + (1 - x_1 - x_2 - y_1)\lambda_1 x_1, \tag{27a}$$
$$\dot{x}_2 = -\mu_2 x_2 + (1 - x_1 - x_2 - y_2)\lambda_2 x_2, \tag{27b}$$
$$\dot{y}_1 = \mu_1 x_1 - \nu_1 y_1 - \lambda_2 x_2 y_1, \tag{27c}$$
$$\dot{y}_2 = \mu_2 x_2 - \nu_2 y_2 - \lambda_1 x_1 y_2, \tag{27d}$$

as illustrated in Fig. 3b. The model is fully determined by six parameters: λ_1, λ_2, μ_1, μ_2, ν_1, and ν_2.

Before starting the analysis of this model, we observe that, because $\nu_1 > 0$ and $\nu_2 > 0$, we can apply Theorem 3, which provides necessary and sufficient conditions for global asymptotic stability of the DFE.

6.1. Results on the boundary endemic equilibria

We start by considering the BEEs, representing survival-of-the-fittest scenarios. While their existence is proved in Proposition 5, here we study their stability. The results of this analysis are summarized in the following theorem.

Theorem 5. *Consider the Waning Virus-specific Immunity Model in Eq. (27). Then, the following conclusions hold:*

1. *If $\lambda_i/\mu_i \leq 1$ for both $i \in \{1, 2\}$, then the DFE is globally asymptotically stable.*

2. *If $\lambda_i/\mu_i > 1$ and $\lambda_j/\mu_j \leq 1$, for $i \neq j \in \{1, 2\}$, then the DFE is unstable. Moreover, there is a unique BEE with*

$$x_i = \frac{\nu_i(\lambda_i - \mu_i)}{\lambda_i(\mu_i + \nu_i)}, \quad y_i = \frac{\mu_i(\lambda_i - \mu_i)}{\lambda_i(\mu_i + \nu_i)}, \quad x_j = y_j = 0, \tag{28}$$

   which is globally asymptotically stable for any initial condition in the interior of the domain.

3. *If $\lambda_i/\mu_i > \lambda_j/\mu_j > 1$, for $i \neq j \in \{1, 2\}$, then the DFE is unstable. Moreover, there are two BEEs, viz.*

$$x_j = \frac{\nu_j(\lambda_j - \mu_j)}{\lambda_j(\mu_j + \nu_j)}, \; y_j = \frac{\mu_j(\lambda_j - \mu_j)}{\lambda_j(\mu_j + \nu_j)}, \; x_i = y_i = 0, \tag{29}$$

   which is always unstable, and that of Eq. (28), which is locally asymptotically stable iff

$$\nu_i > \nu_i^* = \frac{\mu_i \lambda_i(\lambda_j - \mu_j)}{\mu_j(\lambda_i \mu_j - \lambda_j \mu_i)}, \tag{30}$$

   and unstable if $\nu_i < \nu_i^*$.

Proof. Item 1 is a straightforward consequence of Theorem 3. The computation of the BEEs and the assessment of their (local) stability has been performed in [29] through a direct analysis of Eq. (27) and of the eigenvalues of its Jacobian matrix computed in the equilibrium point. For more details, see [29, Theorem 9 and Corollary 11]. This yields item 3, and the first part of item 2. We are left to prove (almost) global convergence for item 2). Without any loss in generality, let us consider the case $\lambda_1/\mu_1 > 1$ and $\lambda_2/\mu_2 < 1$, where the system has only the equilibrium on the boundary Eq. (28) with $x_2 = y_2 = 0$. From Eq. (27b), we observe that $\dot{x}_2 \leq -(\mu_2 - \lambda_2)x_2$. By Gronwall's inequality, $x_2(t) \leq x_2(0)e^{-(\mu_2 - \lambda_2)t}$, and thus it converges exponentially fast to 0. The system is thus a perturbation of a single-virus SIRIS model, which converges exponentially fast to its unique BEE from any initial condition in the interior (see Proposition 3). Hence, the unique BEE is (almost) globally asymptotically stable. □

6.2. Results on the coexistence endemic equilibria

We now study the existence of CEEs, i.e., equilibria in with both viruses are present ($x_1 \neq 0$ and $x_2 \neq 0$). We immediately observe that the results in Theorem 5 preclude the existence of such CEEs for all scenarios, except when $\lambda_1/\mu_1 > 1$ and $\lambda_2/\mu_2 > 1$. In the following, we will focus on this scenario. First, the following result (with proof reported in Appendix C) proves that they cannot exist when one of the BEEs is stable, i.e., when $\nu_i > \nu_i^*$ from Eq. (30).

Proposition 13. *Consider the Waning Virus-specific Immunity Model in Eq. (27) with $\lambda_i/\mu_i > \lambda_j/\mu_j > 1$ and $\nu_i > \nu_i^*$ from Eq. (30). Then, no CEEs can exist.*

A consequence of Proposition 13, is that, when $\lambda_i/\mu_i > \lambda_j/\mu_j > 1$ and $\nu_i > \nu_i^*$, the system has a single (locally) stable equilibrium, for which the simulations in Fig. 2a suggest global asymptotic stability. Evidently, CEEs can only be present when the two BEEs are unstable. The following result (with proof reported in Appendix D) establishes the existence of such equilibria and provide a bound on their number.

Proposition 14. *If $\lambda_i/\mu_i > \lambda_j\mu_j > 1$ and $\nu_i < \nu_i^*$, then, for almost all values of the parameters, the system has either one or three CEEs, with no more than two of them being stable.*

Proposition 14 guarantees the existence of CEEs for the waning virus-specific immunity specialization of our SIRIS model, in the region of the parameter space in which none of the BEEs or the DFE are stable. Such result provides analytical support to the hypothesis in the medical literature that immunity may play a key role in favoring coexistence of multiple competitive diseases [17]. Finally, the numerical simulations in Fig. 5 suggest that, when such CEEs exist, then there is always exactly one of them which is globally asymptotically stable.

7. Conclusion

In this paper, we proposed and analyzed a novel mathematical model for the spread of two competing diseases that accounts for real-world features of natural immunity, including partial virus-specific and cross-immunity protection, and waning immunity. Through the theoretical analysis of the proposed model, termed bivirus SIRIS model,

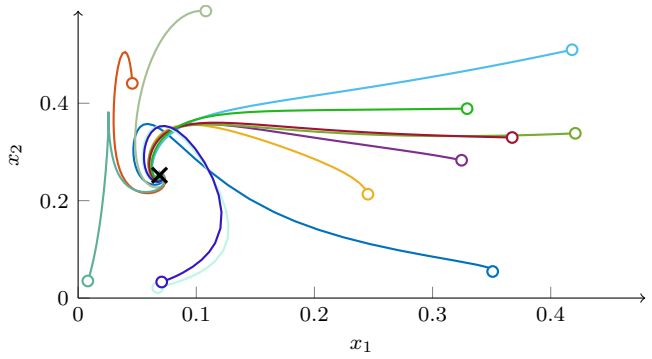

Figure 5: Simulations of Model II with $\lambda_1 = \lambda_2 = 0.7$, $\mu_1 = 0.4$, $\mu_2 = 0.2$, $\nu_1 = \nu_2 = 0.08$, from different initial conditions (colored circles). All trajectories converge to the same CEE, which is denoted with a black cross.

we established general results that characterize the asymptotic behavior of the system in terms of convergence to the disease-free equilibrium or to an endemic state, further characterizing and counting the possible endemic equilibria. Then, we delved into the analysis of two specific implementations of the model, inspired by realistic scenarios, which allowed us to shed light on the impact of partial immunity and waning virus-specific immunity, respectively, on the transient and asymptotic behavior of the system. In particular, we demonstrated how the complex nature of immunity can impact the emergent behavior of an epidemic disease; for instance, by allowing multiple competing diseases to coexist in an endemic equilibrium.

The modeling framework and the results presented in this paper pave the way for several lines of future research. First, our theoretical results provide a thorough characterization of the two specializations of interest. However, the analysis of the most general scenario is limited to establishing conditions for the eradication of both diseases, while in the endemic regime, results are limited to the computation of the winner-take-all endemic equilibria and a characterization of the possible coexistence equilibria. Further effort should be placed into extending the study of the transient and asymptotic behavior of the system to the general bivirus SIRIS model. Second, while our model was implemented in a homogeneous scenario where the individuals of the population interact in an all-to-all fashion, further modeling extensions of the SIRIS framework should be developed and studied toward incorporating heterogeneity across the population and in the pattern of interactions, e.g., by embedding the bivirus model onto a network structure, similar to [14, 24, 27, 28]. Third, leveraging our mathematical formulation of the bivirus model, one can investigate the problem of mitigating an epidemic outbreak by extending the modeling framework to time-variant scenarios, which allows to consider, e.g., closed-loop intervention policies. This would allow us to unveil how the characteristics of natural immunity shape an optimal intervention policy, using, e.g., the methods developed in [4, 25, 26]. Finally, while the features of natural immunity incorporated into our model are based on real-world observations [10–12, 18–22] and the consistency of our results with empirical evidence and epidemiological theories provides some high-level validation to our approach [13, 16, 17], a rigorous validation of the model is still missing and should be performed by establishing systematic ways to match real-world data to our predictions (see, e.g., [39, 40]), building on our theoretical findings.

CRediT authorship contribution statement

Lorenzo Zino: Conceptualization, Methodology, Software, Validation, Formal analysis, Investigation, Resources, Data Curation, Writing — Original Draft, Visualization, Project administration

Mengbin Ye: Conceptualization, Methodology, Formal analysis, Investigation, Resources, Writing — Review & Editing, Funding acquisition

Brian D.O. Anderson: Conceptualization, Methodology, Formal analysis, Investigation, Writing — Review & Editing

Declaration of Competing Interests

The authors declare that they have no known competing financial interests or personal relationships that could have appeared to influence the work reported in this paper.

Data Availability

No data was used for this study.

References

[1] W. Mei, S. Mohagheghi, S. Zampieri, F. Bullo, On the dynamics of deterministic epidemic propagation over networks, Annu. Rev. Control 44 (2017) 116–128.

[2] P. E. Paré, C. L. Beck, T. Başar, Modeling, estimation, and analysis of epidemics over networks: An overview, Annu. Rev. Control 50 (2020) 345–360.

[3] L. Zino, M. Cao, Analysis, prediction, and control of epidemics: A survey from scalar to dynamic network models, IEEE Circuits Syst. Mag. 21 (4) (2021) 4–23.

[4] F. Blanchini, P. Bolzern, P. Colaneri, G. De Nicolao, G. Giordano, Optimal control of compartmental models: The exact solution, Automatica 147 (2023) 110680.

[5] C. Castillo-Chavez, W. Huang, J. Li, Competitive exclusion and coexistence of multiple strains in an SIS STD model, SIAM J. Appl. Math. 59 (1999) 1790–811.

[6] B. A. Prakash, A. Beutel, R. Rosenfeld, C. Faloutsos, Winner takes all: competing viruses or ideas on fair-play networks, in: Proc. 21st Int. Conf. World Wide Web, 2012, pp. 1037–1046.

[7] F. Darabi Sahneh, C. Scoglio, Competitive epidemic spreading over arbitrary multilayer networks, Phys. Rev. E 89 (2014) 062817.

[8] A. Santos, J. M. F. Moura, J. M. F. Xavier, Bi-virus SIS epidemics over networks: Qualitative analysis, IEEE Trans. Netw. Sci. Eng. 2 (1) (2015) 17–29.

[9] M. Ye, B. D. O. Anderson, Competitive epidemic spreading over networks, IEEE Control Syst. Lett. 7 (2023) 545–552.

[10] S. Nickbakhsh, et al., Virus–virus interactions impact the population dynamics of influenza and the common cold, Proc. Natl. Acad. Sci. USA 116 (52) (2019) 27142–27150.
[11] K. F. Chan, L. A. Carolan, D. Korenkov, J. Druce, J. McCaw, P. C. Reading, I. G. Barr, K. L. Laurie, Investigating viral interference between influenza a virus and human respiratory syncytial virus in a ferret model of infection, J. Infect. Dis. 218 (3) (2018) 406–417.
[12] R. Greer, P. McErlean, K. Arden, C. Faux, A. Nitsche, S. Lambert, M. Nissen, T. Sloots, I. Mackay, Do rhinoviruses reduce the probability of viral co-detection during acute respiratory tract infections?, J. Clin. Virol. 45 (1) (2009) 10–15.
[13] E. B. Hodcroft, CoVariants: SARS-CoV-2 Mutations and Variants of Interest, https://covariants.org (2021).
[14] M. Ye, B. D. O. Anderson, J. Liu, Convergence and Equilibria Analysis of a Networked Bivirus Epidemic Model, SIAM Journal of Control and Optimization 60 (2) (2022) S323–S346.
[15] V. Doshi, S. Mallick, D. Y. Eun, Convergence of bi-virus epidemic models with non-linear rates on networks—a monotone dynamical systems approach, IEEE/ACM Trans. Netw. 31 (3) (2023) 1187–1201.
[16] CDC Centers for Disease Control and Prevention, The National Respiratory and Enteric Virus Surveillance System (NREVSS), https://www.cdc.gov/surveillance/nrevss/index.html (2023).
[17] S. Bhattacharyya, P. H. Gesteland, K. Korgenski, O. N. Bjørnstad, F. R. Adler, Cross-immunity between strains explains the dynamical pattern of paramyxoviruses, Proc. Natl. Acad. Sci. USA 112 (43) (2015) 13396–13400.
[18] M. B. Townsend, et al., Humoral immunity to smallpox vaccines and monkeypox virus challenge: Proteomic assessment and clinical correlations, J. Virol. 87 (2) (2013) 900–911.
[19] J. Kaler, A. Hussain, G. Flores, S. Kheiri, D. Desrosiers, Monkeypox: A comprehensive review of transmission, pathogenesis, and manifestation, Cureus 14 (7) (2022).
[20] Y. Goldberg, M. Mandel, Y. M. Bar-On, O. Bodenheimer, L. S. Freedman, N. Ash, S. Alroy-Preis, A. Huppert, R. Milo, Protection and waning of natural and hybrid immunity to SARS-CoV-2, N. Engl. J. Med. 386 (23) (2022) 2201–2212.
[21] X. Ren, J. Zhou, J. Guo, C. Hao, M. Zheng, R. Zhang, Q. Huang, X. Yao, R. Li, Y. Jin, Reinfection in patients with COVID-19: a systematic review, Glob. Health Res. Policy. 7 (1) (2022) 1–20.
[22] A. Iwasaki, What reinfections mean for COVID-19, Lancet Infect. Dis 21 (1) (2021) 3–5.
[23] N. Glanville, S. L. Johnston, Challenges in developing a cross-serotype rhinovirus vaccine, Curr. Opin. Virol. 11 (2015) 83–88.
[24] C. Zhang, S. Gracy, T. Başar, P. E. Paré, A networked competitive multi-virus SIR model: Analysis and observability, in: Proc. 9th NECSYS, 2022, pp. 13–18.
[25] E. Gubar, Q. Zhu, Optimal control of influenza epidemic model with virus mutations, in: Proc. 2013 Eur. Control Conf., 2013, pp. 3125–3130.
[26] V. Taynitskiy, E. Gubar, Q. Zhu, Optimal impulsive control of epidemic spreading of heterogeneous malware, in: Proc. 20th IFAC World Congr., Vol. 50, 2017, pp. 15038–15043.
[27] C. Poletto, S. Meloni, A. V. Metre, V. Colizza, Y. Moreno, A. Vespignani, Characterising two-pathogen competition in spatially structured environments, Sci. Rep. 5 (1) (2015).
[28] D. A. Burbano Lombana, L. Zino, S. Butail, E. Caroppo, Z.-P. Jiang, A. Rizzo, M. Porfiri, Activity-driven network modeling and control of the spread of two concurrent epidemic strains, Appl. Netw. Sci. 7 (1) (2022).
[29] L. Zino, M. Ye, B. D. O. Anderson, On a bi-virus epidemic model with partial and waning immunity, IFAC-PapersOnLine 56 (2) (2023) 83–88, 22nd IFAC World Congress.
[30] B. Pachpatte, Inequalities for Differential and Integral Equations, 1st Edition, Academic Press, San Diego CA, US, 1997.
[31] S. Sastry, Nonlinear systems: Analysis, Stability, and Control, Springer Science & Business Media, 2013.
[32] J. Lee, Introduction to Smooth Manifolds, Springer-Verlag, New York, 2013.
[33] V. Guillemin, A. Pollack, Differential topology, Vol. 370, American Mathematical Soc., 2010.
[34] O. Balmer, M. Tanner, Prevalence and implications of multiple-strain infections, Lancet Infect. Dis. 11 (11) (2011) 868–878.
[35] F. Blanchini, Set invariance in control, Automatica 35 (11) (1999) 1747–1767.
[36] G. Teschl, Ordinary Differential Equations and Dynamical Systems, Vol. 140, American Mathematical Society, Providence, RI, 2012.
[37] D. Angeli, E. D. Sontag, Monotone control systems, IEEE Trans. Automat. Contr. 48 (10) (2003) 1684–1698.
[38] N. N. Krasovskii, Stability of Motion, Stanford University Press, 1963.
[39] J. A. Kopec, et al., Validation of population-based disease simulation models: a review of concepts and methods, BMC Public Health 10 (1) (2010).
[40] K. A. Dautel, E. Agyingi, P. Pathmanathan, Validation framework for epidemiological models with application to COVID-19 models, PLOS Comput. Biol. 19 (3) (2023) e1010968.
[41] J. Hofbauer, An index theorem for dissipative semiflows, Rocky Mt. J. Math. 20 (4) (1990) 1017–1031.

Appendix A. Proof of Lemma 1

Proof. We prove just the first pair of inequalities, the second following by an identical argument. Recall that $w = 1-x_1-x_2-y$ is necessarily nonnegative, corresponding to the fraction of susceptible individuals. Then observe that $\dot{x}_1 = -\mu_1 x_1 + (1-x_1-x_2-(1-\alpha_{11})y)\lambda_1 x_1 = -\mu_1 x_1 + (w+\alpha_{11}y)\lambda_1 x_1 \geq -\mu_1 x_1 + \lambda_1\alpha_{11}(w+y)x_1 = -\mu_1 x_1 + \lambda_1\alpha_{11}(1-x_1-x_2)x_1$. To establish the claim regarding strict inequalities, observe first that the differential equations for x_1, x_2 are of the form $\dot{x}_i = g_i(x_1,x_2,y)x_i$, which means that the conditions $x_1(0) > 0$ and $x_2(0) > 0$ propagate for all time, so that $x_1(t) > 0$ and $x_2(t) > 0$, $\forall t \geq 0$. It is also readily verified using the differential equations for x_1, x_2 and y that $\dot{w} = -(\lambda_1 x_1 + \lambda_2 x_2)w$, which means that the condition $w(0) > 0$ also propagates for all time $t \geq 0$. The differential equation for y shows that for all $t > 0$, $y(t) > 0$, even if $y(0) = 0$. Then in relation to the inequality chain immediately above, since $w(t)$ and $x_1(t)$ are nonzero, and $\alpha_{11} \neq 1$, there holds $(1-\alpha_{11})\lambda_1 w x_1 > 0$ and so the inequality in the above chain is strict. To verify the upper bound, observe that $\dot{x}_2 = -\mu_2 x_2 + (1-x_1-x_2-(1-\alpha_{22})y)\lambda_2 x_2 \leq -\mu_2 x_2 + \lambda_2(1-x_1-x_2)x_2$. Since $\alpha_{22} \neq 1$ and $x_2(t)$ and $y(t)$ are positive, the inequality is also strict. □

Appendix B. Proof of Proposition 12

Proof. The steady state equation for y yields$(\mu_1 - \alpha_{11}\lambda_1 y)x_1 + (\mu_2 - \alpha_{22}\lambda_2 y)x_2 = 0$. The coefficients of x_1 and x_2 in the above equation are both strictly positive, except for the case in which $y = 1$ and $\frac{\alpha_{11}\lambda_1}{\mu_1} = \frac{\alpha_{22}\lambda_2}{\mu_2} = 1$. Hence, the only equilibrium solution in the region of interest requires $x_1 = x_2 = 0$ (note that, when $y = 1$, then this is necessarily verified), but then the equilibrium value of y is unspecified. Note also that $x_1 = x_2 = 0, y \in [0,1]$ defines a line segment of equilibria (as revealed by direct calculation), *irrespective of the inequalities among the parameters.* At such an equilibrium, the Jacobian matrix is

diagonal, with entries equal to $-\mu_1+\lambda_1(1-(1-\alpha_{11})y)$, $-\mu_2+\lambda_2(1-(1-\alpha_{22})y)$, and 0.

The nonsingular part of the Jacobian gives some information. In particular, for the line segment of equilibria defined by $x_1=x_2=0$, there will be an attractive interval defined precisely by those values $\bar{y}$ for which the two nonzero eigenvalues are negative, i.e., $-\mu_1+\lambda_1[1-(1-\alpha_{11})\bar{y}]<0$ and $-\mu_2+\lambda_2[1-(1-\alpha_{22})\bar{y}]<0$, or $\bar{y}>\frac{\lambda_1-\mu_1}{\lambda_1(1-\alpha_{11})}$ and $\bar{y}>\frac{\lambda_2-\mu_2}{\lambda_2(1-\alpha_{22})}$. Obviously, there is also a requirement that $\bar{y}\leq 1$. It is easily verified that the two conditions $\alpha_{11}\lambda_1<\mu_1$ and $\alpha_{22}\lambda_2<\mu_2$ are necessary and sufficient to ensure that $(\lambda_1-\mu_1)/\lambda_1(1-\alpha_{11})<1$ and $(\lambda_2-\mu_2)/\lambda_2(1-\alpha_{22})<1$.

For the cases in which $\alpha_{11}\lambda_1=\mu_1$ or $\alpha_{22}\lambda_2=\mu_2$, we observe that all the equilibria on the line are unstable, except for one with $\bar{y}=1$, whose stability cannot be simply determined by the Jacobian. However, we can easily observe that the equilibrium point $(0,0,1)$ is always attractive in directions orthogonal to the line if $\alpha_{11}\lambda_1\leq\mu_1$ and $\alpha_{22}\lambda_2\leq\mu_2$. In fact, orthogonal to the line segment of equilibria, the dynamics reduces to a bivirus SIS model with infection rates $\tilde{\lambda}_1=\alpha_{11}\lambda_1$ and $\tilde{\lambda}_2=\alpha_{22}\lambda_2$, for which Proposition 3 yields the claim.

Finally, we are left to prove global convergence, which we do by contradiction. Assume that the system does not converge to the healthy manifold $\mathcal{H}$. First, we observe that, since the line segment $y\in(\bar{y},1)\in\mathcal{H}$ is locally attractive, then there exists a positive constant $\delta>0$ such that, if there were to hold $x_1(t)+x_2(t)\leq\delta$ and $y\geq\bar{y}-\delta$, then the trajectory would converge to the line. Since we have assumed that $x(t)$ does not converge to the line, then it must be true that either i) $x_1(t)+x_2(t)>\delta$ or ii) $y<\bar{y}-\delta$, for all $t\geq 0$. In both cases, we can conclude that $1-y(t)>\delta$. Proposition 7, combined with our temporary assumption that the system does not converge to $\mathcal{H}$ guarantees that there exists $\tau_\delta\geq 0$ such that $w(t)\leq\frac{\min\{\alpha_{11},\alpha_{22}\}\delta}{2}$, for any $t\geq\tau_\delta$. Then, using Eq. (19), we bound $\dot{x}_i=-\mu_i x_i+(w+\alpha_{ii}y)\lambda_i x_i\leq-\mu_i x_i+(w+\alpha_{ii}y)\frac{\mu_i}{\alpha_{ii}}x_i=-\mu_i(1-y-\frac{w}{\alpha_{ii}})x_i$, for both $i\in\{1,2\}$. For any $t\geq\tau_\delta$, this implies that $\dot{x}_i\leq-\frac{\mu_1\delta}{2}x_i$. Finally, Gronwall's inequality yields $x_i(t)\leq\exp\{-\frac{\mu_i}{2}\delta(t-\tau_\delta)\}\to 0$, which contradicts our assumption. Consequently, the system should necessarily converge to the healthy manifold. □

Appendix C. Proof of Proposition 13

Proof. Without any loss in generality, we consider $i=1$. A CEE of Eq. (27) is a point $(x_1,x_2,y_1,y_2)\in\mathcal{D}$ such that $x_1>0$, $x_2>0$ and the following four equalities hold:

$$0=-\mu_1+(1-x_1-x_2-y_1)\lambda_1 \tag{C.1a}$$
$$0=-\mu_2+(1-x_1-x_2-y_2)\lambda_2 \tag{C.1b}$$
$$0=\mu_1x_1-\nu_1y_1-\lambda_2x_2y_1 \tag{C.1c}$$
$$0=\mu_2x_2-\nu_2y_2-\lambda_1x_1y_2. \tag{C.1d}$$

In order to prove that no CEEs can exist, we consider the following related system of equations:

$$0=-\mu_1+(1-X_1-X_2-Y_1)\lambda_1, \tag{C.2a}$$
$$0=-\mu_2+(1-X_1-X_2)\lambda_2, \tag{C.2b}$$
$$0=\mu_1X_1-\nu_1Y_1-\lambda_2X_2Y_1, \tag{C.2c}$$

which is obtained from Eqs. (C.1a)–(C.1c), by modifying Eq. (C.1b) through removal of the term $-\lambda_2y_2$. The proof follows two main steps. First, we show that given any solution $(\bar{x}_1,\bar{x}_2,\bar{y}_1,\bar{y}_2)$ of Eq. (C.1) in the domain of interest, and letting $(\bar{X}_1,\bar{X}_2,\bar{Y}_1)$ be any solution of Eq. (C.2) (without restriction to any domain), there necessarily holds $\bar{x}_2\leq\bar{X}_2$. Then, we prove that Eq. (C.2) does not admit solutions with $\bar{X}_2\geq 0$, which in turns implies that there cannot be solutions of Eq. (C.1) with $\bar{x}_2>0$.

Let $(\bar{X}_1,\bar{X}_2,\bar{Y}_1)$ be a solution of Eq. (C.2). From Eq. (C.2b), we obtain that

$$\bar{X}_1+\bar{X}_2=1-\mu_2/\lambda_2. \tag{C.3}$$

In a similar way, from Eq. (C.1b) and using the fact that $\bar{y}_2\geq 0$, we obtain the inequality

$$\bar{x}_1+\bar{x}_2\leq\bar{x}_1+\bar{x}_2+\bar{y}_2=1-\mu_2/\lambda_2=\bar{X}_1+\bar{X}_2. \tag{C.4}$$

Similarly, by comparing the expressions for $\bar{Y}_1$ and $\bar{y}_1$ obtained from the equilibrium specialization of Eq. (C.2a) and Eq. (C.1a), respectively, and inserting the inequality obtained in Eq. (C.4), we conclude that

$$\bar{Y}_1\leq\bar{y}_1. \tag{C.5}$$

Next, we observe that $\bar{Y}_1$ can be explicitly obtained and is positive. By dividing Eq. (C.2a) by λ_1 and Eq. (C.2b) by λ_2, and subtracting the two equations, we get

$$\bar{Y}_1=\frac{\lambda_1\mu_2-\lambda_2\mu_1}{\lambda_1\lambda_2}=\frac{\mu_2}{\lambda_2}-\frac{\mu_1}{\lambda_1}>0 \tag{C.6}$$

with the positivity following by the Proposition hypothesis. In the light of Eq. (C.5), this implies that $\bar{y}_1>0$.

Using the two inequalities Eq. (C.4) and Eq. (C.5) and the positivity of $\bar{Y}_1$ and $\bar{y}_1$, we will now show that $\bar{x}_2\leq\bar{X}_2$. To prove this, assume temporarily to the contrary that there holds $\bar{X}_2<\bar{x}_2$ (and we will prove a contradiction).

From Eq. (C.1c) and Eq. (C.2c), we observe that:

$$\bar{X}_2=\frac{\mu_1\bar{X}_1}{\lambda_2\bar{Y}_1}-\frac{\nu_1}{\lambda_2},\qquad\bar{x}_2=\frac{\mu_1\bar{x}_1}{\lambda_2\bar{y}_1}-\frac{\nu_1}{\lambda_2}, \tag{C.7}$$

where the nonzero nature of $\bar{Y}_1$ and $\bar{y}_1$ is critical. From Eq. (C.4), and with the temporary assumption $\bar{X}_2<\bar{x}_2$, then there would necessarily hold $\bar{X}_1>\bar{x}_1$. Moreover, since $\bar{Y}_1\leq\bar{y}_1$, from Eq. (C.7) we bound (using again the positivity of $\bar{Y}_1$ and $\bar{y}_1$) $\bar{X}_2=\frac{\mu_2\bar{X}_1}{\lambda_2\bar{Y}_1}-\frac{\nu_1}{\lambda_2}\geq\frac{\mu_2\bar{x}_1}{\lambda_2\bar{y}_1}-\frac{\nu_1}{\lambda_2}=\bar{x}_2$, which contradicts our assumption, proving that $\bar{x}_2\leq\bar{X}_2$.

Now, we focus on Eq. (C.2). From Eq. (C.2c), we get

$$\bar{Y}_1=\frac{\mu_1\bar{X}_1}{\nu_1+\lambda_2\bar{X}_2}. \tag{C.8}$$

By equating the right-hand sides of Eq. (C.6) and Eq. (C.8), we obtain $\frac{\lambda_1\mu_2-\lambda_2\mu_1}{\lambda_1\lambda_2} = \frac{\mu_1\bar{X}_1}{\nu_1+\lambda_2\bar{X}_2}$, which implies

$$\nu_1 = \frac{\mu_1\lambda_1\lambda_2\bar{X}_1}{\lambda_1\mu_2-\lambda_2\mu_1} - \lambda_2\bar{X}_2. \tag{C.9}$$

By using the assumption that $\nu_1 > \nu_1^*$, and inserting the expression of ν_1^* from Eq. (30) into Eq. (C.9), we obtain $\frac{\mu_1\lambda_1\lambda_2\bar{X}_1}{\lambda_1\mu_2-\lambda_2\mu_1} - \lambda_2\bar{X}_2 > \frac{\mu_1\lambda_1(\lambda_2-\mu_2)}{\mu_2(\lambda_1\mu_2-\lambda_2\mu_1)}$, which, after some algebraic simplifications, reads

$$\bar{X}_1 > 1 - \frac{\mu_2}{\lambda_2} + \frac{\lambda_1\mu_2-\lambda_2\mu_1}{\mu_1\lambda_1}\bar{X}_2, \tag{C.10}$$

where the coefficient of $\bar{X}_2$ is strictly positive. Finally, inserting Eq. (C.3) into Eq. (C.10), we get $\bar{X}_1 > \bar{X}_1 + \bar{X}_2 + \frac{\lambda_1\mu_2-\lambda_2\mu_1}{\mu_1\lambda_1}\bar{X}_2$, which can only be satisfied if $\bar{X}_2 < 0$, yielding the claim. □

Appendix D. Proof of Proposition 14

Proof. From Eq. (C.1), we observe that, at a CEE, we have $y_1 = \frac{\mu_1 x_1}{\nu_1+\lambda_2 x_2}$ and $y_2 = \frac{\mu_2 x_2}{\nu_2+\lambda_1 x_1}$. When these equations are substituted into the first two equations of Eq. (C.1), there results two quadratic equations in x_1, x_2:

$$\begin{aligned}&\lambda_1\lambda_2 x_1x_2 + \lambda_1\lambda_2 x_2^2 + \lambda_1(\mu_1+\nu_1)x_1\\ &\quad + (\mu_1\lambda_2 + \nu_1\lambda_1 - \lambda_1\lambda_2)x_2 + \nu_1(\mu_1-\lambda_1) = 0 \qquad \text{(D.1)}\\ &\lambda_1\lambda_2 x_1^2 + \lambda_1\lambda_2 x_1x_2 + (\mu_2\lambda_1 + \nu_2\lambda_2 - \lambda_1\lambda_2)x_1\\ &\quad + \lambda_2(\nu_2+\mu_2)x_2 + \nu_2(\mu_2-\lambda_2) = 0 \qquad \text{(D.2)}\end{aligned}$$

From Eq. (D.1), we obtain

$$x_1 = \frac{-\lambda_1\lambda_2 x_2^2 - (\mu_1\lambda_2 + \nu_1\lambda_1 - \lambda_1\lambda_2)x_2 + \nu_1(\lambda_1-\mu_1)}{\lambda_1\lambda_2 x_2 + \lambda_1(\mu_1+\nu_1)}. \tag{D.3}$$

When this equation is substituted into Eq. (D.2), algebraic simplifications leads to a third order equation, which has at least one and at most three real solutions.

To prove existence of at least one solution in the domain of interest, we observe that Eq. (27) is such that i) $\mathbf{R}_+^n$ is forward invariant ($x_i = 0 \Leftarrow f_i(x) \geq 0$), and ii) the semiflow induced by the system is dissipative, i.e., $\limsup_{t\to+\infty} x_i(t) \leq k$ for some constant $k > 0$. As a consequence, we can use the theory developed in [41]. A key result of this theory states that for a given system satisfying those two aforementioned properties, there exists at least one saturated equilibrium [41, Theorem 2], whose definition is explainable as follows. Without loss of generality, let $\bar{x} = [0, 0, \ldots, \bar{x}_{k+1}, \ldots, \bar{x}_n]^\top$, with $k \geq 0$ and $\bar{x}_i > 0$ for $i \geq k+1$. In other words, $\bar{x}$ is a equilibrium where the first k entries are equal to 0. The Jacobian of $\bar{x}$ can be expressed as

$$J(\bar{x}) = \begin{bmatrix} A & \mathbf{0} \\ B & C \end{bmatrix}, \tag{D.4}$$

where A is a Metzler matrix. We call A the external part of the Jacobian, and C the internal part. Define $s(A)$ as the spectral abscissa of a given matrix A. Then, $\bar{x}$ is said to be an unsaturated equilibrium if $s(A) > 0$, a saturated equilibrium if $s(A) \leq 0$ and a strictly saturated equilibrium if $s(A) < 0$. If $\bar{x} > \mathbf{0}_n$, i.e., it is a positive vector, then $\bar{x}$ is always saturated.

If $\lambda_i/\mu_i > \lambda_j\mu_j > 1$ and $\nu_i < \nu_i^*$, the system has three equilibria other than the (possibly existing) co-existence ones. Evidently, the DFE is unstable, and thus the origin is an unsaturated equilibrium. Next, consider the BEE $(0, \bar{x}_2, 0, \bar{y}_2)$. After a permutation, the Jacobian can be written into the form of Eq. (D.4), which yields

$$\bar{J} = \begin{bmatrix} -\mu_1 + (1-x_2)\lambda_1 & 0 & 0 & 0 \\ \mu_1 & -\lambda_2 x_2 - \nu_1 & 0 & 0 \\ \lambda_2 x_2 & 0 & -\lambda_2 x_2 & -\lambda_2 x_2 \\ -\lambda_1 y_2 & 0 & \mu_2 & -\nu_2 \end{bmatrix}. \tag{D.5}$$

The block corresponding to C in Eq. (D.4) is Hurwitz; the block corresponding to A is lower-triangular with the entry $-\lambda_2 x_2 - \nu_1 < 0$, and $-\mu_1 + (1-x_2)\lambda_1$ being positive or negative according as $(0, \bar{x}_2, 0, \bar{y}_2)$ is unstable or locally stable, respectively. In other words, $(0, \bar{x}_2, 0, \bar{y}_2)$ is a strictly saturated equilibrium iff it is locally exponentially stable, and it is an unsaturated equilibrium if it is unstable. The same statement can be made about the other BEE, $(\bar{x}_1, 0, \bar{y}_1, 0)$. According to [41, Theorem 2], this implies that when both BEEs are unstable, there exists at least one CEE, as none of the BEEs or the healthy equilibrium are saturated. Finally, Proposition 6 guarantees that all CEEs are nondegenerate for almost all choices of the parameters (see Remark 3 for the fact that setting $\alpha_{11} = \alpha_{22} = 1$ and $\alpha_{12} = \alpha_{21} = 0$ is not restrictive). This implies that all saturated equilibria are nondegenerate. Hence, [41, Theorem 2] guarantees that the sum of the indices of the saturated fixed points is equal to $+1$, where the index of a fixed point is equal to the sign of the determinant of the negative of the Jacobian matrix evaluated at the fixed point. As a consequence, stable equilibria necessarily have index $+1$, while unstable equilibria can have index $+1$ or -1 (depending on the number of positive eigenvalues). Consequently, in order for the sum of the indices to be equal to $+1$, either there is a unique equilibrium (with index $+1$) or there are three equilibria (two with index $+1$ and one with index -1), yielding the claim. □